Eleven million years of arc volcanism at the Aucanquilcha Volcanic Cluster, northern Chilean Andes: implications for the life span and emplacement of plutons

Anita L. Grunder, Erik W. Klemetti, Todd C. Feeley and Claire M. McKee

ABSTRACT: The arid climate of the Altiplano has preserved a volcanic history of ∼11 million years at the Aucanquilcha Volcanic Cluster (AVC), northern Chile, which is built on thick continental crust. The AVC has a systematic temporal, spatial, compositional and mineralogical development shared by other long-lived volcanic complexes, indicating a common pattern in continental magmatism with implications for the development of underlying plutonic complexes, that in turn create batholiths.

The AVC is a ∼700-km^2, Tertiary to Recent cluster of at least 19 volcanoes that have erupted andesite and dacite lavas (∼55 to 68 wt.% SiO_2) and a small ash-flow tuff, totalling 327 ± 20 km^3. Forty $^{40}Ar/^{39}Ar$ ages for the AVC range from $10·97 \pm 0·35$ to $0·24 \pm 0·05$ Ma and define three major 1·5 to 3 million-year pulses of volcanism followed by the present pulse expressed as Volcán Aucanquilcha. The first stage of activity (∼11–8 Ma, Alconcha Group) produced seven volcanoes and the 2-km^3 Ujina ignimbrite and is a crudely bimodal suite of pyroxene andesite and dacite. After a possible two million year hiatus, the second stage of volcanism (∼6–4 Ma, Gordo Group) produced at least five volcanoes ranging from pyroxene andesite to dacite. The third stage (∼4–2 Ma, Polan Group) represents a voluminous pulse of activity, with eruption of at least another five volcanoes, broadly distributed in the centre of the AVC, and composed dominantly of biotite amphibole dacite; andesites at this stage occur as magmatic inclusions. The most recent activity (1 Ma to recent) is in the centre of the AVC at Volcán Aucanquilcha, a potentially active composite volcano made of biotite-amphibole dacite with andesite and dacite magmatic inclusions.

These successive eruptive groups describe (1) a spatial pattern of volcanism from peripheral to central, (2) a corresponding change from compositionally diverse andesite-dacite volcanism to compositionally increasingly restricted and increasingly silicic dacite, (3) a change from early anhydrous mafic silicate assemblages (pyroxene dominant) to later biotite amphibole dacite, (4) an abrupt increase in eruption rate; and (5) the onset of pervasive hydrothermal alteration.

The evolutionary succession of the 327-km^3 AVC is similar to other long-lived intermediate volcanic complexes of very different volumes, e.g., eastern Nevada (thousands of km^3, Gans et al. 1989; Grunder 1995), Yanacocha, Perú (tens of km^3, Longo 2005), and the San Juan Volcanic System (tens of thousands of km^3, Lipman 2007) and finds an analogue in the 10-m.y. history and incremental growth of the Cretaceous Tuolumne Intrusive Suite (Coleman et al. 2004; Glazner et al. 2004). The present authors interpret the AVC to reflect episodic sampling of the protracted and fitful development of an integrated and silicic middle to upper crustal magma reservoir over a period of at least 11 million years.

KEY WORDS: Argon geochronology, batholith, Chile, eruption rates

Studies of the timescales of magmatic systems have recently focused on short timescales of magmatic evolution (days to 10^5 years), fuelled by developments in measuring uranium-series isotopes (e.g., Reid et al. 1997; Bacon et al. 2000; Cooper et al. 2001; Lowenstern et al. 2000; Zellmer et al. 2000). Although short-term processes are vital to developing accurate models of magma batches and crystal histories, longer timescales need to be considered for the evolution of volcanic and plutonic complexes and the integration of magmatic processes at a crustal scale.

A fundamental problem in studying continental arc magmatism is the interpretation of the architecture of large plutonic complexes found in many ancient arcs. Batholithic suites like the Sierra Nevada Batholith or the Coastal Batholith of Peru grow episodically over many tens of millions of years and are made of many plutonic complexes, that is batholiths within a batholith (e.g., Evernden & Kistler 1970; Pitcher 1978; Ducea 2001). Despite their apparent homogeneity, such plutonic complexes are made of multiple intrusions emplaced over the course of many hundreds of thousands to millions of years (e.g., McNulty et al.1996; Wiebe 1996; Dilles & Wright 1988; Glazner et al. 2004). Work on the Tatoosh Plutonic Complex, Washington (Mattinson 1977), the Tuolumne Intrusive Suite, California (Coleman et al. 2004; Glazner et al. 2004), and the Potrerillos District, Chile (Marsh et al. 1997) has extended the potential life span of plutonic complexes to ∼10 Ma. The similarly long-lived San Juan Volcanic Field of Colorado is the most frequently cited work of protracted volcanism, providing a window into the development of batholiths (Lipman 1984, 2000, 2007). However, little work has been done to identify modern volcanic systems in continental arc settings that could be the volcanic equivalent to long-lived plutonic systems. The
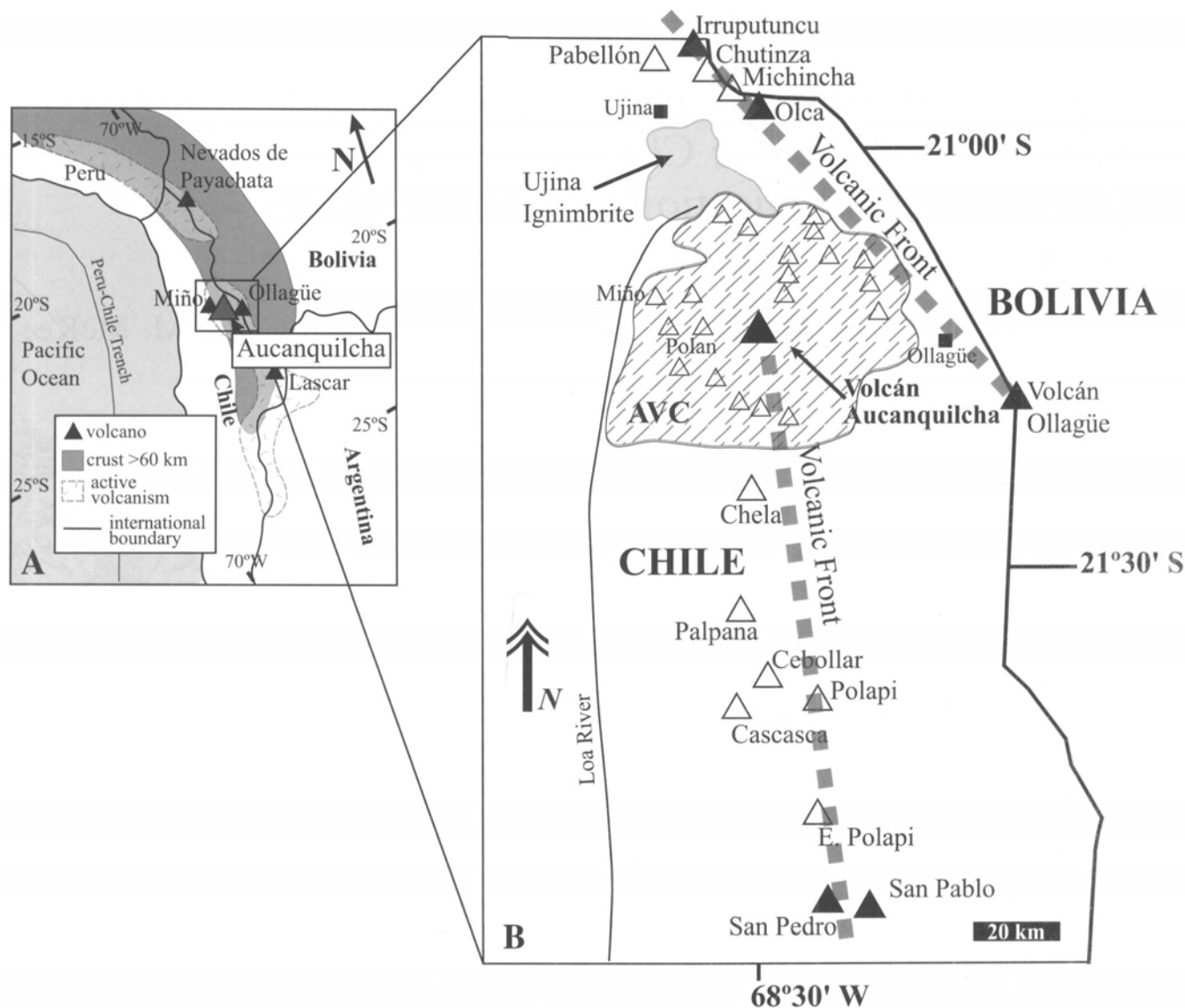
Figure 1 (A) Location map for the Aucanquilcha Volcanic Cluster relative to the western coast of South America and the Perú-Chile trench. Four other volcanoes that have been the subject of study in the region are shown for reference. (B) Regional location of the AVC (dashed area) and Ujina Ignimbrite (shaded) and composite volcanoes (triangles). Volcanoes designated as active (de Silva & Francis 1991) are solid triangles. Extinct volcanoes are designated by an open triangle. Solid squares represent settlements. The grey dashed line delineates the alignment of the active volcanic arc in the Central Andes.

Aucanquilcha Volcanic Cluster of the central Andes provides a volcanic sampling of crustal magmatism occurring in one area for ~11 million years and its temporal evolution has implications for the assembly of a plutonic complex, or batholith.

The present study deconstructs the magmatic history of the Aucanquilcha Volcanic Cluster (AVC), located in the Central Volcanic Zone of the northern Chilean Andes (21°S). The cluster is made up of at least 19 volcanic centres that lie within a ~700 km^2 region between the Loa River and the Chilean-Bolivian border near Ollagüe (Fig. 1). Arid conditions since the Miocene (Galli-Oliver 1967) have allowed preservation of volcanic edifices, thereby providing access to a long record of volcanism.

The results of mapping, forty ^{40}Ar/^{39}Ar dates, and geochemical analyses of samples from the Aucanquilcha Volcanic Cluster are presented. Eruptive volumes are also reconstructed for all major centres of the cluster to determine the rates of eruption over its history and compare the temporal, compositional and mineralogical evolution of the Aucanquilcha Volcanic Cluster to other long-lived continental magmatic systems.

1. Tectonic setting and geologic background

1.1. The Central Andes and Aucanquilcha Volcanic Cluster

The Aucanquilcha Volcanic Cluster (AVC) lies in the central of three active volcanic zones along the Andean margin of South America (Fig. 1). The Central Volcanic Zone (CVZ) is marked by extreme crustal thickness, in excess of 60 km (Zandt *et al.* 1994; Trumbull *et al.*1999) and is noted for volcanic rocks that have been affected by crustal contamination; rocks have elevated δ^{18}O (7 to 13‰), high ^{87}Sr/^{86}Sr (0·705 to 0·708), and low ε_{Nd} (− 2 to − 8) (e.g., Déruelle *et al.* 1983; Harmon *et al.* 1984; Davidson *et al.* 1991; Wörner *et al.* 1994). The NW-trending belt of late Cenozoic volcanoes that comprise the CVZ includes over 1100 volcanic centres. CVZ volcanic edifices, including those of the Aucanquilcha Volcanic Cluster, are mainly composed of metaluminous, medium-to-high K calc-alkaline andesite and dacite (Fig. 4, Table 2). The AVC is located at an offset in the volcanic front (Fig. 1) and at a transition in Pb-isotope provinces, with less radiogenic

Pb-isotopic character to the south (Wörner *et al.* 1992). Davidson *et al.* (1990) proposed that the crustal isotopic character of CVZ volcanoes resulted from deep crustal contamination of magmas derived from depleted asthenospheric mantle. Alternatively, mantle causes have been postulated. James (1981) proposed extensive recycling of crustal and (or) sedimentary material into the mantle, and Rogers & Hawkesworth (1989) argued for involvement of enriched subcontinental lithospheric mantle. Distinction between the degree of crustal recycling compared to new magmatic input from the mantle to the crust is essential to evaluating crustal growth, as in the case of Cretaceous plutonism in the Sierra Nevada Batholith, where the same debates arise (Wenner & Coleman 2004; Kistler *et al.* 1986).

The CVZ is dominated by compound volcanoes that are underlain by extensive mid-Tertiary ignimbrite deposits (de Silva 1989). Both styles of volcanism have been active since the mid-Miocene, although ignimbrite activity has declined since 10 Ma (Baker 1981). In total, more than 3000 km^3 of volcanic material have been erupted between 21°S and 22°S in the Central Andes during the past 28 Ma (Baker & Francis 1978), yielding a volcanic output rate of ~0·11 km^3/ka.

Crustal thickening has been occurring along the Central Andes, and specifically the Altiplano–Puna Complex, for at least 20 Ma based on palaeobotanical studies (Gregory-Wodzicki 2000), with no more than half of the current elevation attained by 10·7 Ma. Anomalously low seismic velocities occur between depths of ~20 km and 40 km at 21°S (Wigger *et al.*1994; Graeber & Asch 1999), coincident with zones of attenuation of p-wave velocities (Haberland & Rietbrock 2001) and high electrical conductivity (Schwarz & Krüger 1997). Schilling *et al.* (1997) and Schmitz *et al.* (1997) attribute slightly lower crustal density to a zone of interconnecting partial melts at depths of 15–40 km. This is in agreement with the heat flow measurements (Giese 1994). The mid-crustal seismic attenuation zone extends to the south, underlying the extensive Altiplano–Puna Volcanic Complex (Chmielowski *et al.* 1999), and is likely the present day expression of a developing mid-crustal batholith. The AVC lies at the northern margin of the Altiplano–Puna Volcanic Complex.

2. Methods

2.1. Field work
Mapping and sampling of the Aucanquilcha Volcanic Cluster occurred over three field seasons in 1999 and 2000 using 1:50 000 topographic maps and air photo coverage at similar scale. Sampling was aimed at obtaining the oldest and youngest volcanic rocks from each volcanic centre as well as the compositional and mineralogical range. Access is via a network of roads built for the sulphur mining on Volcán Aucanquilcha and Cerro Polan; mining was active until the mid-1990s. Detailed sampling was focused on Volcán Aucanquilcha and Volcán Miño. Mineralogical modes for the volcanic rocks were determined from hand sample and by petrography.

2.2. Geochemical analysis
A total of 168 samples were powdered using an alumina mill and analysed in the GeoAnalytical Lab at Washington State University-Pullman using methods from Johnson *et al.* (1999). The precision for these analyses is <1% for most elements with the exception of Y, Nb and Cr, which are estimated at <5%. 75 samples were analysed for rare earth elements using inductively coupled plasma mass spectrometry (ICP-MS) analyses, performed in the GeoAnalytical Lab at Washington State University using a Sciex Elan 250 ICP-MS. One acid blank and three standard (BCR-P, GMP-01 and MON-01) were run with each set of unknowns. Samples were powdered in a steel shatterbox swing mill and then digested using methods modified from Crock & Lichte (1982) See Klemetti (2005) for details.

Ten samples from Volcán Miño were analysed by instrumental neutron activation analysis for trace elements. Samples were crushed in an alumina shatterbox and then irradiated and analysed at the Oregon State University Triga Reactor facility following the procedure of Laul (1979).

2.3. ^{40}Ar/^{39}Ar age determination
Forty samples were crushed and separated to yield plagioclase, biotite and (or) groundmass. Plagioclase crystals were washed in a dilute HF to remove excess glass. Biotite and groundmass were washed in distilled water. All separates were handpicked to ensure purity. Samples (~100 mg) were then wrapped in Cu-foil, loaded into quartz vials and sealed in standard Al tubes. The tubes were irradiated at the Triga Reactor, Oregon State University.
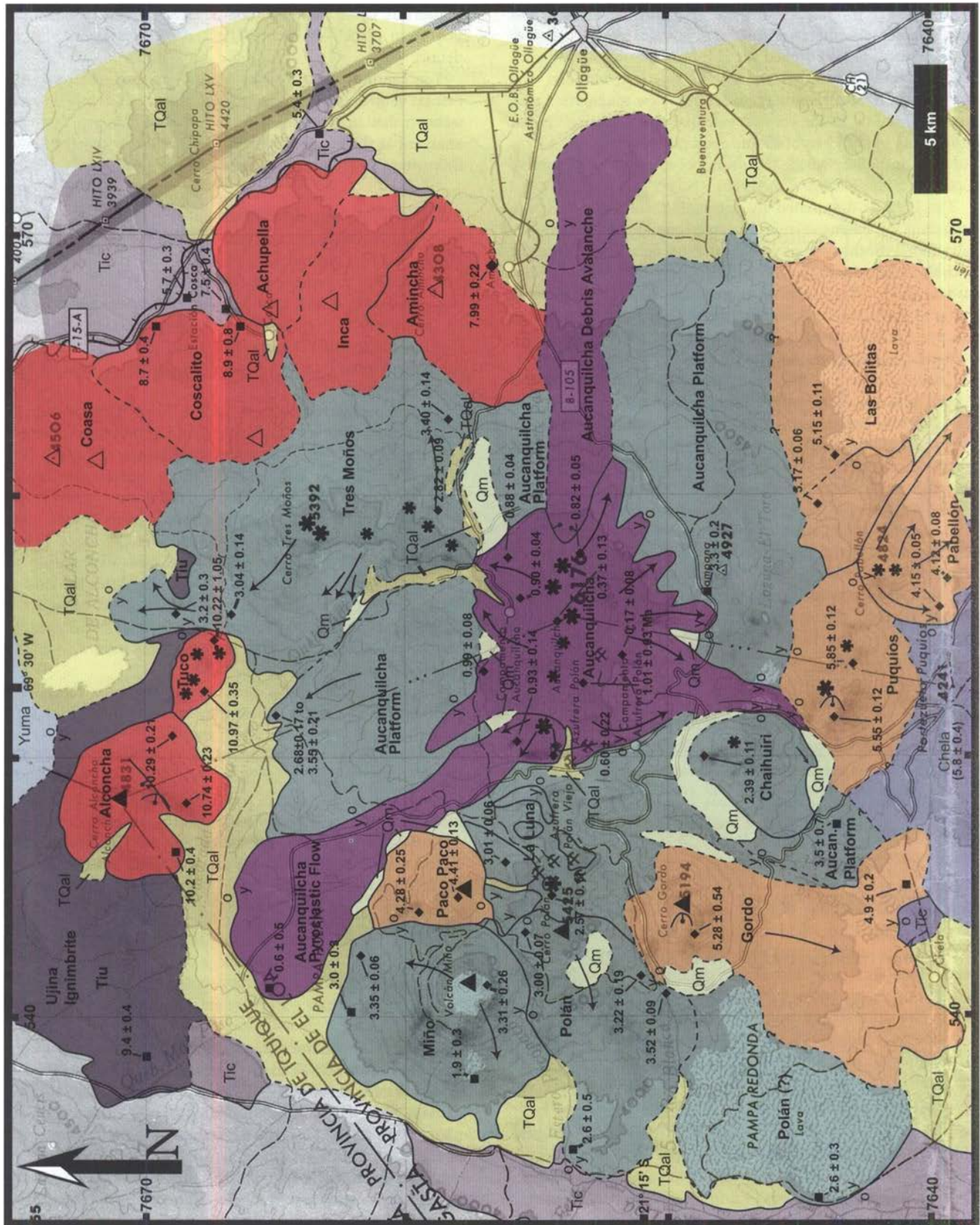
All samples were analysed using a MAP 215′–50 rare gas mass spectrometer at the Noble Gas Laboratory, College of Oceanographic and Atmospheric Sciences, Oregon State University. Ar gas was released using incremental heating methods from Duncan & Hogan (1994) in a temperature-controlled resistance furnace or using a laser system. Laser analyses were done with a Merchantek 10W CO$_2$ laser. Masses 35–40 and intervening baselines were measured during ten sweeps with <10% peak decay per analysis. After the isotopic measurements were made, ages were calculated using ArAr-Calc V2.2 (Koppers 2002), correcting for blanks between 2–4 blanks per analysis, typically at room temperature, ~800°C, ~1100°C and ~1400°C.

Conventional isochron ages are preferred for the ages of each centre (Table 1) when they meet two criteria: (1) a majority of the steps fall along the ^{40}Ar/^{36}Ar-^{39}Ar/^{36}Ar isochron; and (2) the mean standard weighted deviation (MSWD) is below 2·5. When these criteria are not met, the weighted plateau age is used if: (1) the MSWD is below 2·5; (2) the plateau contained at least 3 heating steps; and (3) greater than 50% of ^{39}Ar is released in the steps that comprise the plateau. In the rare case where neither method could meet all criteria, the method with the lowest MSWD was chosen. Most isochron and plateau ages agree within 2 σ error. Preferred ages are highlighted in bold in Table 1.

3. Results

3.1. Overview of the Aucanquilcha Volcanic Cluster
The Aucanquilcha Volcanic Cluster is defined by a subcircular grouping of volcanoes flanked to the west, north and east by alluvial plains, ignimbrite plateau and salt flats that lie at about 4000 m (Fig. 2). The southern edge of the AVC is drawn at the inferred contact with Cerro Chela. The highest part of the AVC is the east-west ridge of Volcán Aucanquilcha, that lies in the centre and has four peaks over 6000 m. The deposits of the AVC volcanoes are mainly blocky andesite and dacite lavas, with sparse pyroclastic material. Mapping delineates 18 volcanic edifices in the AVC, most of which have multiple vents. Abundant evidence of modest Quaternary glaciation in the AVC includes moraines and glacially striated surfaces that decorate centres at elevations above ~4500 m (Fig. 2).
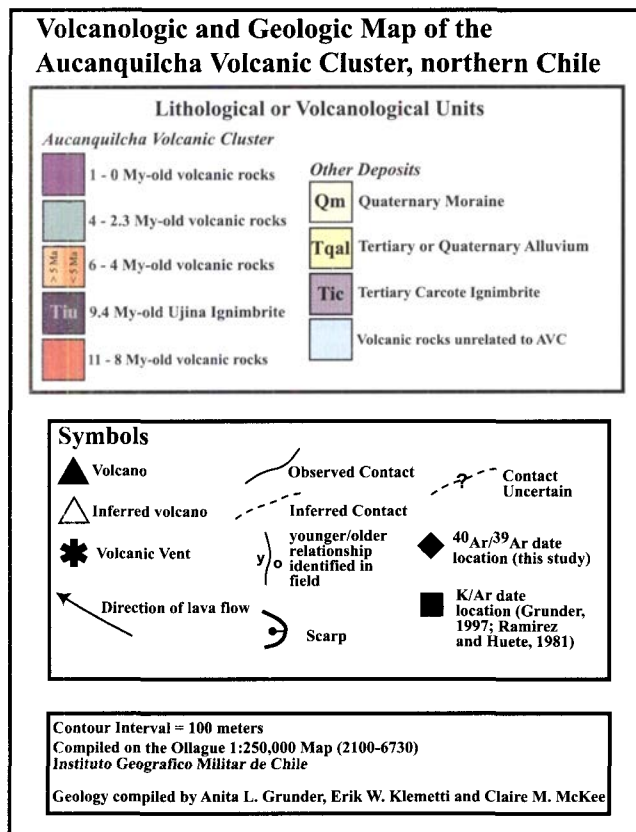
Volcanologic and Geologic Map of the Aucanquilcha Volcanic Cluster, northern Chile

Lithological or Volcanological Units

Aucanquilcha Volcanic Cluster

- 1 - 0 My-old volcanic rocks
- 4 - 2.3 My-old volcanic rocks
- 6 - 4 My-old volcanic rocks
- 9.4 My-old Ujina Ignimbrite
- 11 - 8 My-old volcanic rocks

Other Deposits

- **Qm** Quaternary Moraine
- **Tqal** Tertiary or Quaternary Alluvium
- **Tic** Tertiary Carcote Ignimbrite
- Volcanic rocks unrelated to AVC

Symbols

- ▲ Volcano
- △ Inferred volcano
- ✳ Volcanic Vent
- Direction of lava flow
- Observed Contact
- Inferred Contact
- y/o younger/older relationship identified in field
- Scarp
- Contact Uncertain
- ◆ $^{40}Ar/^{39}Ar$ date location (this study)
- ■ K/Ar date location (Grunder, 1997; Ramirez and Huete, 1981)

Contour Interval = 100 meters
Compiled on the Ollague 1:250,000 Map (2100-6730)
Instituto Geografico Militar de Chile

Geology compiled by Anita L. Grunder, Erik W. Klemetti and Claire M. McKee

Figure 2 Simplified Geologic Map of the Aucanquilcha Volcanic Cluster compiled at 1:250 000. See key for full description of symbols and colour scheme for the mapped area. The Aucanquilcha debris avalanche deposit is remapped (2007) as lavas overridden by the Ollague avalanche deposits.

Forty $^{40}Ar/^{39}Ar$ ages for the AVC range from 10.97 ± 0.35 to 0.24 ± 0.05 Ma define four major, one to three million-year pulses of volcanism (Table 1; Figs 3, 7). The first pulse (~ 11–8 Ma, Alconcha Group) produced seven volcanoes, and probably the 2-km^3 Ujina ignimbrite. This group is a crudely bimodal pyroxene andesite and dacite suite (Figs 4, 5). After a possible two million year hiatus, the second pulse of volcanism (~ 6–4 Ma, Gordo Group) produced at least five volcanoes ranging from pyroxene andesite to dacite. The third pulse (~ 4–2 Ma, Polán Group) represents the most vigorous activity in the history of the AVC, with eruption of at least another six volcanoes broadly distributed in the centre of the AVC, and composed dominantly of biotite-two amphibole dacite. The most recent activity (since ~ 1 Ma) is in the centre of the AVC at Volcán Aucanquilcha, which is a compound volcano made mainly of biotite- two amphibole dacite. Volcán Aucanquilcha is considered potentially active (de Silva & Francis 1991), owing to its youthful morphology and faint steam emission in defunct sulphur mine workings near the summit.

These successive eruptive groups of the AVC describe (1) a spatial pattern of volcanism from peripheral to central (Fig. 2); (2) a change from compositionally diverse volcanism, ranging from basaltic andesite to rhyodacite, to a more limited and increasingly silicic in range (Figs 5, 6); (3) a change from early anhydrous mafic silicate assemblages (pyroxene dominant) to later biotite and amphibole; (4) an abrupt increase in eruption rate (Figs 7, 9); and (5) the onset of pervasive hydrothermal alteration.

3.2. Composition and mineralogy of AVC ejecta

The lavas and minor pyroclastic rocks of the Aucanquilcha Volcanic Cluster range from 55 to 68 wt.% SiO_2 and are

mainly andesite and dacite (Fig. 4). Crystal contents are typically 15 to 35%, but as great as 50%, with plagioclase dominant. Quenched magmatic inclusions are aphanitic or fine grained and range from basaltic andesite to silicic andesite. Coarse phenocrysts (larger than 5 mm) are most common in dacite. Glomerocrysts are common and subordinate to phenocrysts. Textural complexity in minerals, particularly plagioclase, is the rule. Clinopyroxenes occur in virtually all samples, as individual crystals and also commonly in clots with opaque oxides. Orthopyroxene is less abundant than clinopyroxene on the whole. Amphiboles, when present, occur as apparent equilibrium phenocrysts, as well as in various states of reaction, from having opacite rims to thick gabbroic overgrowths; multiple textural varieties occur in single samples. Biotite is common only among young dacites (Fig. 5). Sparse olivine occurs in some mafic samples; sparse quartz and alkali feldspar occur in some felsic samples. Opaque oxides are ubiquitous and zircon and apatite are common accessory minerals.

Trace element patterns of the AVC ejecta are typical of continental arc suites with a pronounced negative Nb anomaly and elevated concentration in large-ion lithophile elements (Fig. 6). Elemental concentrations are diverse early and become more restricted in range in successive groups (Figs 5, 6). The two older groups, Alconcha and Gordo, encompass the entire bulk compositional range. These groups also have large ion lithophile and heavy rare earth elements (HREE) concentrations spanning nearly the entire range for the AVC (Fig. 6). The Gordo Group is bit more restricted in compositional range than the Alconcha Group. The Polan Group has still more silicic and restricted composition. The Polan Group is dominantly made of dacite to silicic andesite lavas, some of which have andesitic inclusions. Polan dacites occupy the upper range of concentration for incompatible elements. The final Aucanquilcha Group is the most evolved of the AVC. It is composed mainly of dacite lavas with silicic andesite inclusions. Compared to the Polan group, the Aucanquilcha group dacites are somewhat depleted in Th, U and HREE, implicating accessory phase effects in differentiation.

Volcán Pabellón and Volcán Miño are set apart (Fig. 5c, d). Volcán Pabellón, the youngest of the Gordo Group, is transitional in character between the Gordo and Polan Groups. Like other Gordo Group volcanoes, it is made of both andesite lavas and dacite, but like the Polan Group, dacite is dominant and andesite occurs as magmatic inclusions. Volcán Miño, a member of the Polan Group, is separated because it lies on the periphery of the distribution of Polan centres and it is composed mainly of andesite lavas.

3.3. Alconcha Group (11 to 8 Ma)

The Alconcha Group is made up of the two composite cones on the northern side of the AVC, Cerro Alconcha, and Volcán Tuco, and a string of five endogenous dome and flow complexes in the northeast sector (Fig. 2). Together, their compositions span from 55 to 68 wt.% SiO_2 (Fig. 5a; Table 2). Alconcha and Tuco, the oldest AVC centres, are substantially eroded, leading to lower peak elevations and smaller footprints compared to more recent volcanoes.

Volcán Tuco (Cerro Garage), yielded two analytically indistinguishable ages at 10.96 ± 0.17 and 10.51 ± 0.72 Ma. Andesite dikes that crop out on the eastern side of the edifice strike north-south, but the vents and edifice generally define a northwest trend that includes Cerro Alconcha. Tuco andesites have plagioclase>clinopyroxene>orthopyroxene=olivine, and dacites have plagioclase>amphibole>clinopyroxene.

Lava and scoria deposits of Cerro Alconcha overlie Volcán Tuco at the col between them. Cerro Alconcha has a great breach in its crater open to the south. Whilst no debris

Table 1 $^{40}Ar/^{39}Ar$ ages for the Aucanquilcha Volcanic Cluster.

Sample	Centre	Material	Coordinates		Total fusion age (Ma)	Isochron age (Ma)	Isochron MSWD	$^{40}Ar/^{39}Ar^1$	Points filled	Plateau age (Ma)[2]	Plateau MSWD	Plateau %39Ar
			N	E								
AP-00-17	Tuco	Plag.	7667·5	552·2	14·05 ± 1·08	**10·97 ± 0·35**	2·16	3·66 ± 0·11	4/7	10·96 ± 0·17	1·78	74·4
AP-00-04	Alconcha	WR	7667·8	547·7	11·03 ± 0·21	**10·78 ± 0·23**	0·31	3·54 ± 0·06	7/9	10·93 ± 0·13	0·71	97·6
AP-00-12	Tuco	Plag.	7667·2	554·3	16·50 ± 7·61	**10·51 ± 0·72**	0·68	5·34 ± 2·46	4/7	11·08 ± 0·66	1·95	**51·9**
AP-00-01	Alconcha	WR core	7667·9	549·4	10·32 ± 0·08	10·29 ± 0·20	0·99	3·32 ± 0·01	3/8	**10·43 ± 0·09**	2·02	68·5
AP-00-82	Amincha	Plag.	7656·1	561·2	8·05 ± 0·20	**8·01 ± 0·19**	1·31	3·07 ± 0·05	6/9	8·04 ± 0·18	1·33	91
AP2-00-42	Puquíos	GM	7643·2	554·2	5·83 ± 0·09	5·96 ± 0·42	1·92	2·21 ± 0·03	4/12	**5·81 ± 0·12**	1·64	**61·2**
AP-00-94	Puquíos	WR	7643·5	551·5	5·65 ± 0·11	**5·28 ± 0·11**	1·81	1·83 ± 0·03	5/9	5·36 ± 0·11	3·55	**47**
AP2-00-84	Las Bolitas	GM	7643·2	559·2	5·43 ± 0·05	**5·23 ± 0·09**	0·23	1·99 ± 0·01	6/11	5·21 ± 0·05	0·16	85·8
AP2-00-88	Las Bolitas	GM	7643·0	560·6	5·30 ± 0·05	**5·13 ± 0·18**	0·26	1·98 ± 0·01	3/9	5·32 ± 0·08	3·02	68
AP-00-85	Gordo	WR	7648·8	542·0	5·95 ± 0·48	4·43 ± 3·82	1·28	1·91 ± 0·15	6/8	**5·49 ± 0·46**	1·12	82·4
AP-00-37	Paco Paco	Plag.	7658·5	543·6	5·71 ± 0·21	**4·41 ± 0·11**	0·89	1·83 ± 0·07	4/8	4·49 ± 0·09	1·96	**71·9**
AP-00-38	Paco Paco	WR	7659·5	544·1	5·52 ± 0·48	**4·26 ± 0·26**	0·26	1·77 ± 0·15	4/9	4·27 ± 0·14	0·18	**86**
AP2-00-03	Pabellón	GM	7659·4	556·1	4·23 ± 0·05	4·26 ± 0·18	0·07	1·62 ± 0·02	4/12	**4·14 ± 0·05**	0·64	**81**
AP2-00-01	Pabellón	GM	7658·8	556·5	4·22 ± 0·08	3·95 ± 0·31	1·14	1·25 ± 0·10	7/11	**4·12 ± 0·08**	1·24	**89·5**
AP-00-64	Tres Monos	Plag.	7658·8	559·4	5·72 ± 1·47	**3·88 ± 1·59**	2·13	1·95 ± 0·50	4/7	4·73 ± 1·04	2·70	**55**
VM99-10	Miño	Amph.	7662·0	543·0	4·31 ± 0·27	3·78 ± 0·47	0·60	1·58 ± 0·10	4/8	**3·54 ± 0·17**	0·31	51
AP-00-08	Aucan. Ptfm.	Plag.	7662·6	551·3	3·62 ± 0·13	**3·59 ± 0·17**	0·43	1·16 ± 0·04	5/7	3·66 ± 0·11	0·60	81·4
AP-00-73	Polan	GM	7650·2	541·6	3·57 ± 0·05	3·52 ± 0·09	1·60	1·25 ± 0·01	3/9	**3·50 ± 0·05**	1·05	**52·3**
AP-00-65	Tres Monos	Plag.	7658·4	563·0	4·50 ± 0·73	**3·40 ± 0·14**	1·36	1·44 ± 0·23	6/8	3·43 ± 0·08	1·13	**84·0**
AP-00-74	Polan	Plag.	7650·7	541·7	5·02 ± 0·11	**3·36 ± 0·07**	0·03	1·82 ± 0·03	3/8	3·36 ± 0·06	0·01	**35**
VM99-10	Miño	GM	7662·0	543·0	3·07 ± 0·08	3·34 ± 0·06	1·42	1·05 ± 0·03	5/9	**3·35 ± 0·04**	1·17	51·9
VM99-52	Miño	Plag.	7656·8	541·1	3·83 ± 0·12	3·31 ± 0·26	0·14	1·31 ± 0·10	4/8	**3·31 ± 0·09**	0·09	65·51
AP-00-14	Tres Monos	Plag.	7667·0	554·7	3·74 ± 0·33	**3·04 ± 0·14**	2·22	1·22 ± 0·10	4/7	3·07 ± 0·07	1·63	**71·6**
AP-00-50	Polan	WR core	7655·6	543·2	3·13 ± 0·04	**3·00 ± 0·07**	0·38	1·01 ± 0·01	4/8	3·00 ± 0·03	0·26	**57·8**
AP-00-49	La Luna	Plag.	7656·2	546·1	3·03 ± 0·06	**2·97 ± 0·05**	0·58	0·97 ± 0·02	7/9	2·95 ± 0·04	0·58	84·2
AP-00-64	Tres Monos	Biotite	7658·8	559·4	3·03 ± 0·09	**2·83 ± 0·09**	0·49	1·09 ± 0·03	4/8	2·89 ± 0·07	1·18	**84·9**
AP-00-14	Tres Monos	GM	7667·0	554·7	2·77 ± 0·04	2·78 ± 0·12	0·25	0·96 ± 0·01	3/8	**2·78 ± 0·04**	0·13	**90·1**
AP-00-08	Aucan. Ptfm.	Biotite	7662·6	551·3	2·71 ± 0·04	**2·68 ± 0·17**	1·25	0·95 ± 0·01	7/10	2·70 ± 0·04	1·18	80·1
AP-00-52	La Luna	Plag.	7654·5	544·8	2·83 ± 0·08	**2·57 ± 0·11**	0	0·99 ± 0·03	4/7	2·65 ± 0·05	0·93	83·4
AP-00-76A	Chaihuiri	Biotite	7648·4	550·2	2·45 ± 0·04	2·32 ± 0·13	0·02	0·78 ± 0·01	3/8	**2·39 ± 0·04**	0·65	83
AP-600-92	Aucanquilcha	Plag.	7655·2	550·5	1·46 ± 0·09	1·28 ± 0·50	1·83	0·52 ± 0·03	3/9	**1·02 ± 0·11**	1·89	53·2
AP-00-46	Aucanquilcha	Biotite	7653·0	553·4	1·08 ± 0·02	1·02 ± 0·06	0·58	0·36 ± 0·01	4/9	**1·04 ± 0·01**	0·55	93·3
AP-00-54	Aucanquilcha	Biotite	7655·5	556·2	1·10 ± 0·05	**0·98 ± 0·04**	0·64	0·38 ± 0·01	7/8	1·02 ± 0·03	1·51	98
AP-00-81	Aucanquilcha	Plag.	7650·9	561·2	1·17 ± 0·08	0·96 ± 0·07	0·75	0·21 ± 0·01	5/8	**0·92 ± 0·04**	0·95	87
AP-600-64	Aucanquilcha	GM	7655·5	555·3	0·95 ± 0·01	**0·91 ± 0·04**	0·04	0·33 ± 0·01	4/8	0·95 ± 0·02	1·33	67·5
AP-600-68	Aucanquilcha	Plag.	7656·2	557·8	1·14 ± 0·03	0·88 ± 0·04	0·15	0·42 ± 0·01	5/8	**0·89 ± 0·03**	0·94	57
AP-600-100	Aucanquilcha	Plag.	7653·3	557·7	1·28 ± 0·06	0·83 ± 0·13	1·79	0·45 ± 0·02	3/9	**0·89 ± 0·06**	1·96	54·6
AP-00-77	Aucanquilcha	Plag.	7646·1	551·8	1·20 ± 0·09	0·62 ± 0·41	3·63	0·21 ± 0·02	3/9	**0·66 ± 0·10**	1·72	**58**
AP-00-28	Aucanquilcha	Plag.	7654·8	549·8	0·79 ± 0·09	**0·47 ± 0·07**	0·55	0·28 ± 0·03	6/9	0·61 ± 0·11	6·37	**88·8**
AP-600-51	Aucanquilcha	Plag.	7651·6	553·8	0·45 ± 0·05	0·19 ± 0·09	0·23	0·16 ± 0·02	5/8	**0·24 ± 0·05**	0·77	**72·4**
AP-600-60	Aucanquilcha	GM	7653·7	555·4	1·09 ± 0·17	0·15 ± 0·25	0	0·37 ± 0·06	3/9	**0·33 ± 0·08**	1·27	59·0

Preferred ages are listed in bold type. Abbreviations for material are as follows: WR core=whole rock core; WR=whole rock; plag.=plagioclase; GM=groundmass; amph=amphibole. All errors are listed as 2σ. Aucan. Ptfm=Aucanquilcha Platform.

avalanche deposits are preserved, a landslide block within the amphitheatre suggests that catastrophic collapse and avalanche deposits are likely to be covered by younger volcanic deposits and alluvium. Lavas from deep in the wall of the breach yield $^{40}Ar/^{39}Ar$ ages of $10·78 ± 0·23$ and $10·43 ± 0·09$ Ma, which overlap with a previous K-Ar age of $10·2 ± 0·4$ (Grunder 1997) for a stratigraphically high sample (Figs 2, 3). Cerro Alconcha lavas have a typical mafic mineralogy of clinopyroxene>orthopyroxene with little to no olivine (in contrast to Tuco); minor amphibole occurs in dacitic samples.

The 9·4-m.y. Ujina Ignimbrite (Ramirez & Huete 1981) laps onto the northern slopes of Tuco and Alconcha. The ignimbrite fills the basin under the town of Ujina, northwest of the AVC (Fig. 2). In much of the outcrop area the ignimbrite is densely welded and has exposed thickness as great as 20 m near the base of Cerro Alconcha, and decreases in thickness and in degree of welding on the northern and western margins of the Ujina basin. The Ujina Ignimbrite is included in the Alconcha Group because of its similar age and composition, and because its distribution suggests a nearby source (Fig. 2; Table 2); the source is not known. The ignimbrite is brown and has 15–20% crystals composed of dominant plagioclase minor alkali feldspar (Vergara 1978) and about 5% mafic minerals, with clinopyroxene>opacite rimmed amphibole>anhedral biotite with opacite rims.

Activity shifted to the east with the formation of five andesite-to-dacite dome complexes in a rough NNW array spanning from Coasa to Cerro Amincha (Figs 2, 5a). Little is known about the four northernmost domes; two dates for Coscalito indicate an age of between 8·7 and 8·9 Ma (Ramirez & Huete 1981) and the $5·6 ± 0·4$ Ma Carcote rhyolite ignimbrite (K-Ar age of Baker 1977) banks against the eastern side
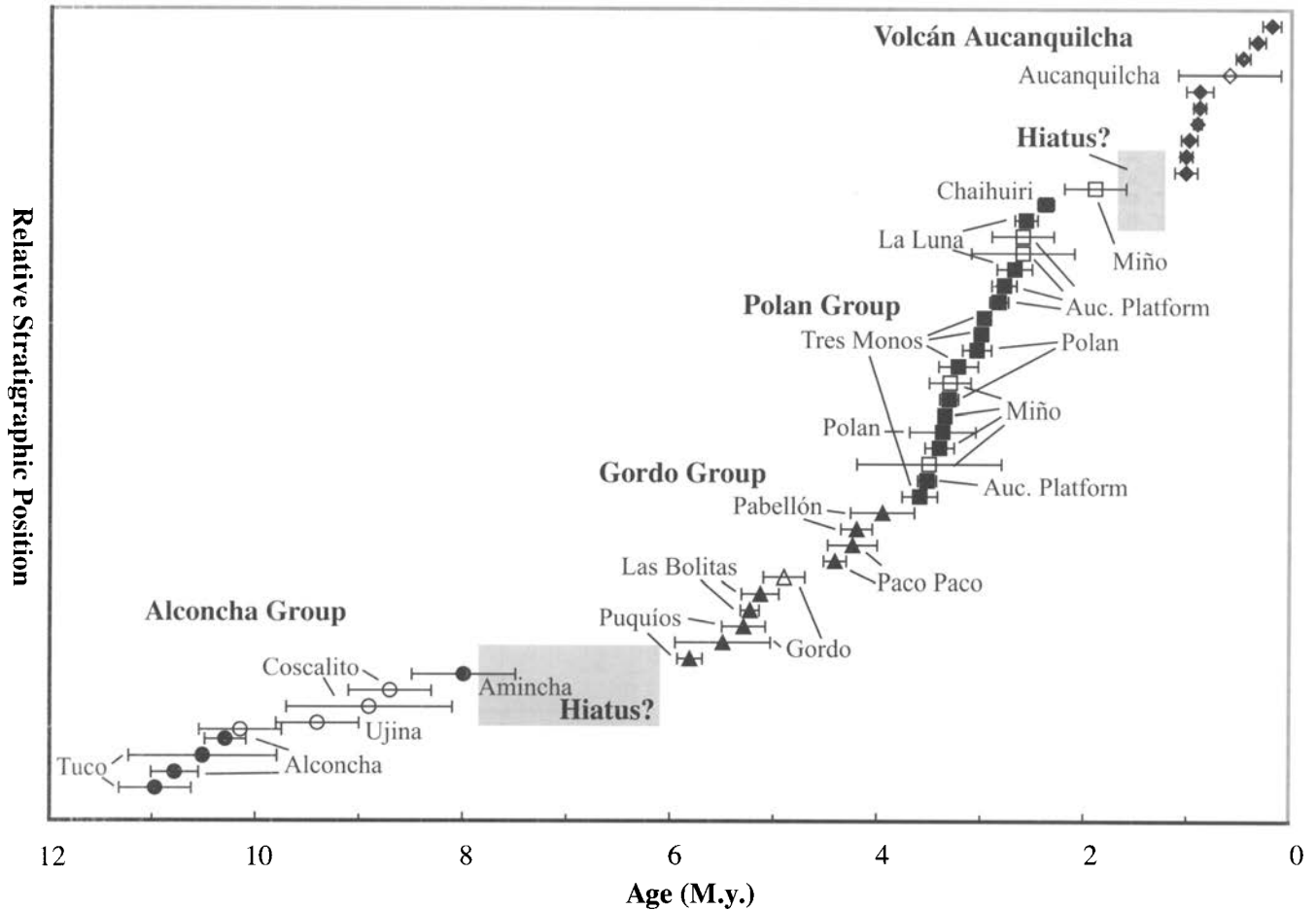
Figure 3 Compilation of age and relative stratigraphic position for the AVC. Clusters in age and geographic grouping lead to definition of the Alconcha, Gordo, Polan and Aucanquilcha groups, coded as circles, triangles, squares and diamonds, respectively. Possible breaks in volcanic activity are indicated by the shaded intervals. These may reflect gaps in sampling. Filled symbols are data from the present study. Open symbols are K-Ar ages from Ramirez and Huete (1981) and Grunder (1997). Ages are shown with 2σ error bars.

of the string of domes. These domes are largely unsampled. Cerro Amincha, yields an age of $8·01 \pm 0·19$ Ma (Table 1) and clinopyroxene as the dominant mafic mineral.

3.4. Gordo Group (6 to 4 Ma)
The Alconcha Group was followed by a shift in volcanism to the Gordo Group, a set of volcanoes mainly along the southern margin of the AVC (Fig. 2). The Gordo Group includes the volcanoes Cerro Puquíos-Cerro Negro ($5·81 \pm 0·21$ to $5·28 \pm 0·11$ Ma), Cerro Gordo ($5·49 \pm 0·46$ Ma), and Cerro Paco Paco ($4·41 \pm 0·09$ to $4·27 \pm 0·14$ Ma), and Volcán Pabellón ($4·1$ Ma), which yield a compositional range of 57 to 66 wt.% SiO_2 (Fig. 5b; Table 2).

The large field of lava flows west of Cerro Gordo yielded an age of $4·9 \pm 0·2$ Ma, and is assigned to Gordo because flow directions are consistent with a vent near Cerro Gordo and the lavas overlie the Carcote ignimbrite. The Las Bolitas lava field ($5·13 \pm 0·18$ to $5·23 \pm 0·09$ Ma) is assigned to the Gordo Group owing to its age and location; vents for the field have not been identified.

Cerro Puquíos and Cerro Negro form a ~6-km NW-trending ridge along the southern side of the AVC. The two overlapping volcanoes, grouped as Puquíos (Fig. 2), have sizeable NE facing glacial cirques exposing interlayered thin lavas and scoria. Cerro Puquíos is slightly younger and has a small amphitheatre in its western flank. Puquíos ejecta typically have plagioclase>clinopyroxene>orthopyroxene>olivine with rare occurrence of amphibole.

Cerro Gordo is one of the larger centres in the AVC. It has a breached crater open to the west, but no related debris avalanche deposits have been found. The breach exposes about a dozen crudely radial dikes. Lavas and dikes are characterised by plagioclase>clinopyroxene>olivine>orthopyroxene>amphibole. Amphibole, while typically a percent or less, is ubiquitous, trace biotite occurs in only one sample.

Volcán Paco Paco, located to the north of most Gordo Group volcanoes (Fig. 2), is a ~4-km diameter stratocone composed of thin agglutinated lavas interlayered with scoria beds that dip steeply from the central crater that is filled with a thick lava. Paco Paco lavas are mainly crystal-poor with sparse, but distinctive olivine subordinate to plagioclase and clinopyroxene and rare amphibole. The late, crater-filling lava is more crystal-rich and the most silicic.

Towards the end of the Gordo Group activity, Volcán Pabellón began to erupt on the southeastern flanks of the Cerro Puquíos and Cerro Negro ridge (Fig. 2). Volcán Pabellón lavas yield ages of between $4·14 \pm 0·05$ and $4·12 \pm 0·08$ Ma (Table 1); it is the first AVC centre to exhibit abundant quenched magmatic inclusions. Mineralogically, Pabellón has an assemblage of plagioclase>clinopyroxene>orthopyroxene>amphibole assemblage with minor biotite and olivine.

3.5. Polan Group (~4 to 2 Ma)
The Polan Group is a series of composite volcanoes and lava flows that have yielded ages from $3·6$ Ma to $2·3$ Ma (Table 1) and that are distributed throughout the central part of the
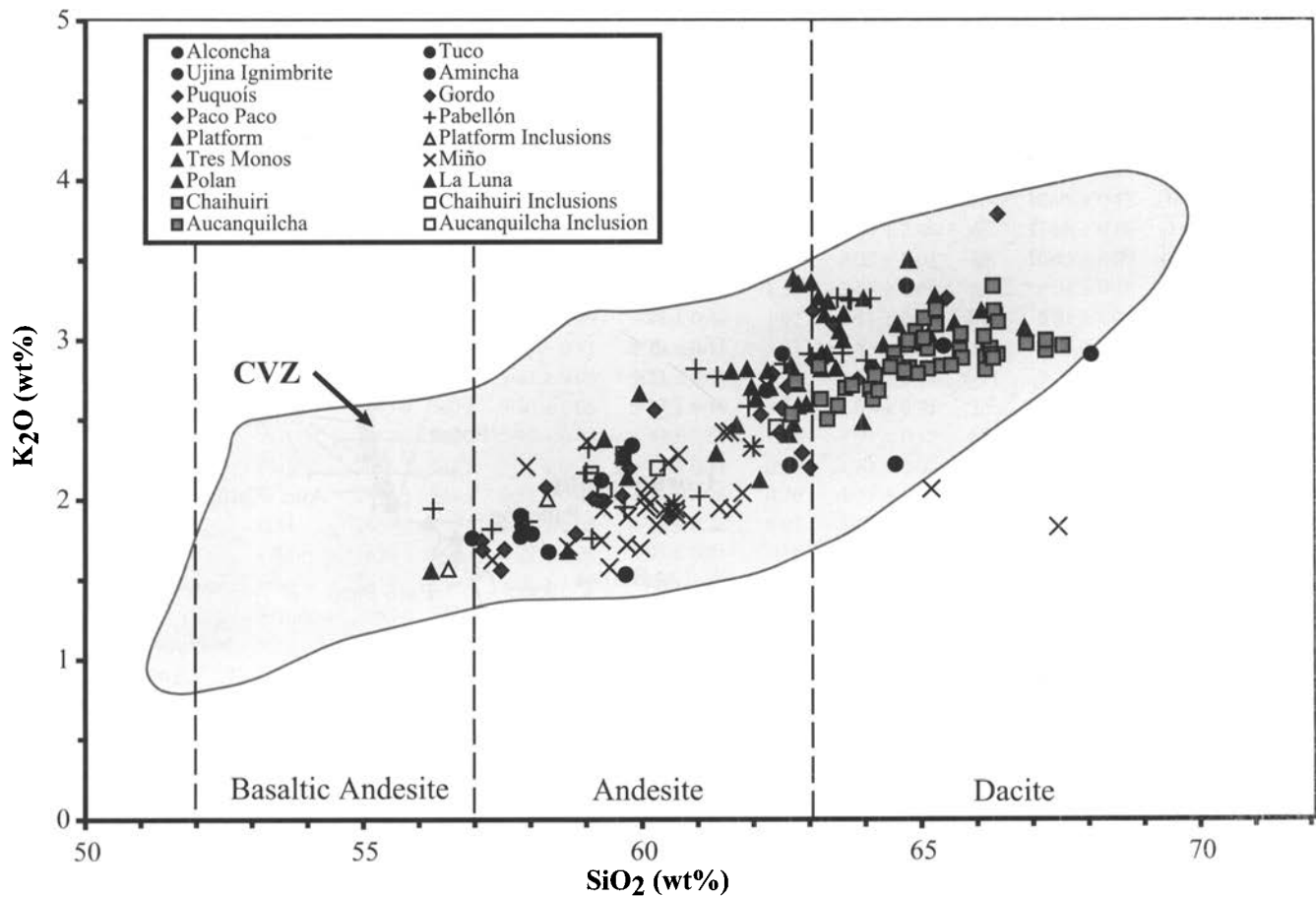
Figure 4   Silica versus K₂O for the AVC compared to the Central Volcanic Zone. Data are normalised to 100% volatile free. The shaded field represents the range for the CVZ compiled from Déruelle *et al.* (1995), Wörner *et al.* (1994, 1988), de Silva *et al.* (1994), Feeley & Davidson (1994), Richards & Villeneuve (2001) and Costa & Singer (2002). Classification boundaries (dashed lines) on silica axis from LeBas *et al.* (1986); trachy-fields omitted.

AVC. The Polan Group represents the largest outpouring of lavas in the cluster and includes the centres Tres Monos, La Luna Cerro Polan, and Chaihuiri, as well as lavas of the Aucanquilcha Platform. Cerro Polan and La Luna fall on an east–west array that presages the east–west alignment of Aucanquilcha itself. In contrast, Tres Monos is made of a series of vents aligned north–south. Volcán Miño, a 3·3 Ma-old (Table 1) andesite cone, formed on the westernmost periphery of the AVC (Fig. 2). Including Volcán Miño, the Polan Group ranges in composition from 56 to 67 wt.% SiO₂, but most samples have between 61 and 65 wt.% SiO₂ (Fig. 5e; Table 2).

The main edifice of Cerro Polan yields ages ranging from between 3·5 ± 0·05 to 3·00 ± 0·03 Ma (Table 1). Flow directions in lava fields to the west and southwest suggest Polan as the source region. A K-Ar date along the western edges of one lava field is 2·6 ± 0·05 Ma (QG-81; Grunder 1997). Lavas from Polan have a plagioclase>clinopyroxene>orthopyroxene> amphibole>biotite assemblage. Polan is deeply incised on its eastern side and the deep exposures are strongly altered.

The La Luna centre lies just east of Polan and both are likely part of a larger pervasively altered compound volcano. La Luna is distinguished by a dome surrounded by a glaciated table of unaltered lava, which caps pervasively altered rock. Ages from the lava tableland and from the La Luna dome are 2·97 ± 0·05 and 2·57 ± 0·11 Ma, overlapping in age with activity at Polan, and constrain some of the alteration to older than ~3 Ma. La Luna samples have subequal clinopyroxene and orthopyroxene>biotite.

The north-striking linear array of at least six vents that make up the three overlapping edifices of Cerro Tres Monos

define a ~14-km ridge at a near right angle to the vent alignment of Volcán Aucanquilcha–La Luna–Polan. Ages from fresh Cerro Tres Monos lava flows indicate activity between 3·40 ± 0·14 and 2·78 ± 0·04 Ma (Table 1) suggesting a life span of ~0·4 to 0·8 m.y. One older age, 3·88 ± 1·59 Ma, has such low precision that it encompasses the range of the other age data and is not used here. Lavas and pyroclastic fall deposits from the Tres Monos ridge are locally hydrothermally altered. Lateral and terminal moraine deposits are particularly well preserved on the western side of the ridge. Tres Monos lavas have more hydrous phases compared to Polan and La Luna; the typical assemblage is plagioclase>clinopyroxene> hornblende>biotite>orthopyroxene.

The Aucanquilcha Platform crops out around Volcán Aucanquilcha (Fig. 2) and presumably underlies it. To the north of Aucanquilcha, the platform lavas yield ages of ~2·7 and 3·6 Ma (Table 1) and have well-defined levees and flow fronts indicating flow to the north from vents now buried by Volcán Aucanquilcha. On the south side of Volcán Aucanquilcha, the platform is mainly a high glaciated shelf that breaks at about 4500 m. Dips of flow bases indicate flow away from Aucanquilcha. Cerro Campana, a small hill to the south of Volcán Aucanquilcha, has a K-Ar age of 3·3 ± 0·2 Ma (Ramirez & Huete 1981), so a large portion of the platform lavas was likely erupted around 2·7 to 3·6 Ma. The Aucanquilcha Platform makes up nearly one third of the estimated volume of the AVC and probably represents several edifices, part of which were eroded by glaciation and part of which are covered. The present authors speculate that the edifice(s) that delivered the lavas of the Aucanquilcha Platform made up an
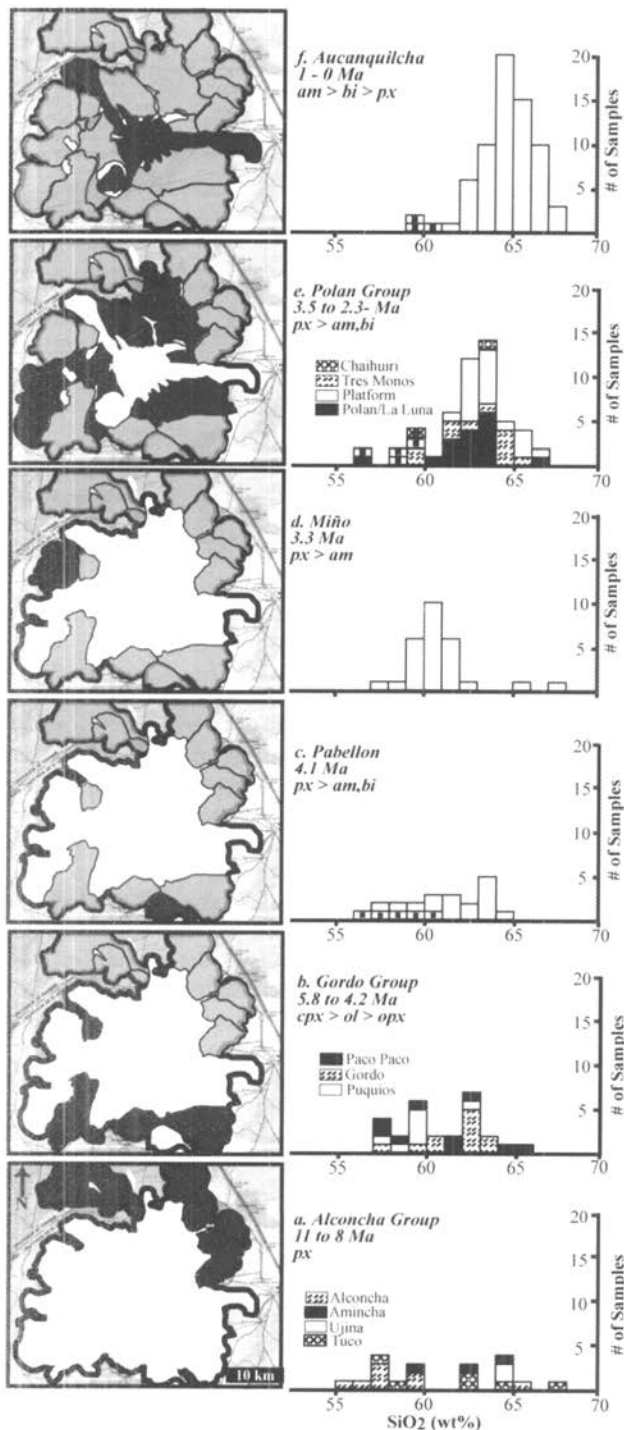
Figure 5 Compositional and mineralogical changes through time at the AVC. Histograms indicate the range of silica for samples of each volcano and are plotted as temporal groups along with maps showing the group's outcrop area and the general mineralogical character of the group. Very sparse or accessory phases are not indicated. Small black squares indicate that the sample is a mafic inclusion: (a) Alconcha Group; (b) Gordo group; (c) Cerro Pabellón, shown separately from the rest of the Gordo group, because it spans a wide range in composition and marks a temporal transition between andesite as lavas (earlier) and andesite as mafic inclusions (later); (d) Volcán Miño, plotted separately from its age group (Polan) because it is peripheral and compositionally intermediate between the andesite common in older groups and dacite that dominate younger centres. (e) Polan group; (f) Aucanquilcha. Mineral abbreviations as follows: (px) pyroxene; (ol) olivine; (am) amphibole (undifferentiated); (hb) hornblende; (pg) pargasite; (bi) biotite. Plagioclase is ubiquitous. Quartz and scarce alkali feldspar occur in some of the most silicic compositions.

east-west ridge now under Volcán Aucanquilcha, extending the Polan-Luna trend. They cannot preclude that the Aucanquilcha Platform covers older centres, such as ejecta of Gordo age (equivalent to the Las Bolitas field) in the southwestern sector of the AVC. The modal mineralogy of the Aucanquilcha platform lavas is typically plagioclase>clinopyroxene≥ orthopyroxene>hornblende>biotite.

The youngest member of the Polan Group, Volcán Chaihuiri, is a dacite dome from which emanate two short flows. Chaihuiri yielded an age of 2.39 ± 0.04 Ma (Table 1). One lava sample has plagioclase biotite>amphibole>clinopyroxene> orthopyroxene and also bears quartz. Extensive moraine deposits occur on the flanks of Chaihuiri.

3.6. Volcán Miño (3·3 Ma)

Volcán Miño is a steep-sided symmetrical cone reaching 5611 m on the westernmost edge of the AVC. The lavas appear to have been fed primarily from a summit vent. Lavas extend to the head of the Loa River to the west, where they overlie volcaniclastic sediments over the Carcote Ignimbrite. Most of the activity at Miño is bracketed by lavas between 3.54 ± 0.17 and 3.31 ± 0.09 Ma (Table 1). Two K-Ar ages for Miño (Grunder 1997) include a flow on the north flank of the volcano at 3.0 ± 0.3 Ma and a relatively young-looking flow on the west flank at 1.9 ± 0.3. Most Volcán Miño lavas range in SiO$_2$ from 59 to 62 wt.% (Fig. 5d; Table 2), a composition uncommon in other centres of the AVC. The modal mineralogy is typically plagioclase>orthopyroxene>clinopyroxene> hornblende with minor olivine in a few samples; rare quartz with clinopyroxene coronae occurs throughout the suite. Although subordinate in abundance, amphibole is conspicuous and has a variety of textures, ranging from equilibrium phenocrysts to crystals with thin opacite rims to crystals with thick disequilibrium reaction textures (McKee 2001). Unlike the rest of the Polan Group, biotite is absent.

3.7. Volcán Aucanquilcha (<1 Ma)

Volcán Aucanquilcha (Figs 2, 5f) is a large compound volcano that developed as a series of overlapping vents in an 8-km, east-west array. Ages for Aucanquilcha Volcano range from 1.04 ± 0.01 Ma to 0.24 ± 0.05 Ma (Table 1), spanning four eruptive stages that are neither spatially nor compositionally systematic in time (Klemetti & Grunder 2008). Large portions of the edifice, especially on the western side, have been pervasively hydrothermally altered. Covellite is reported to occur in fumarolic areas of the summit (Clark 1970). Lavas range in SiO$_2$ from 62·6 to 67·2 wt.%, with most around 64–66 wt.% (Table 2; Fig. 5f).

Volcán Aucanquilcha mainly erupted dacite flows a few km long and one 9-km-long lava on it southern side; it produced one 10-km long, block and ash flow deposit on its western side and a debris avalanche deposit on its eastern side (Fig. 2). Based on the age of the dome source and a block within the flow deposit, the pyroclastic flow occurred at about 0·6 Ma (Klemetti & Grunder 2008). On the eastern flank of the Aucanquilcha edifice, debris avalanche deposits extends ~17 km from a steep scarp just below the summit in 0·9-Ma lavas to the Salar de San Martin O Carcote (Fig. 2). This ~30 km^2 flow has the hummocky terrane at its distal end distinctive of debris avalanches, like the one at nearby Volcán Ollagüe (Feeley et al. 1993).

Overall, Aucanquilcha is the most silicic centre of the AVC and has the highest occurrence of hydrous minerals. Quenched magmatic inclusions are common in most lavas from Aucanquilcha and make up as many as 15 vol.% in some flows. Aucanquilcha is dominated by an assemblage of plagioclase>
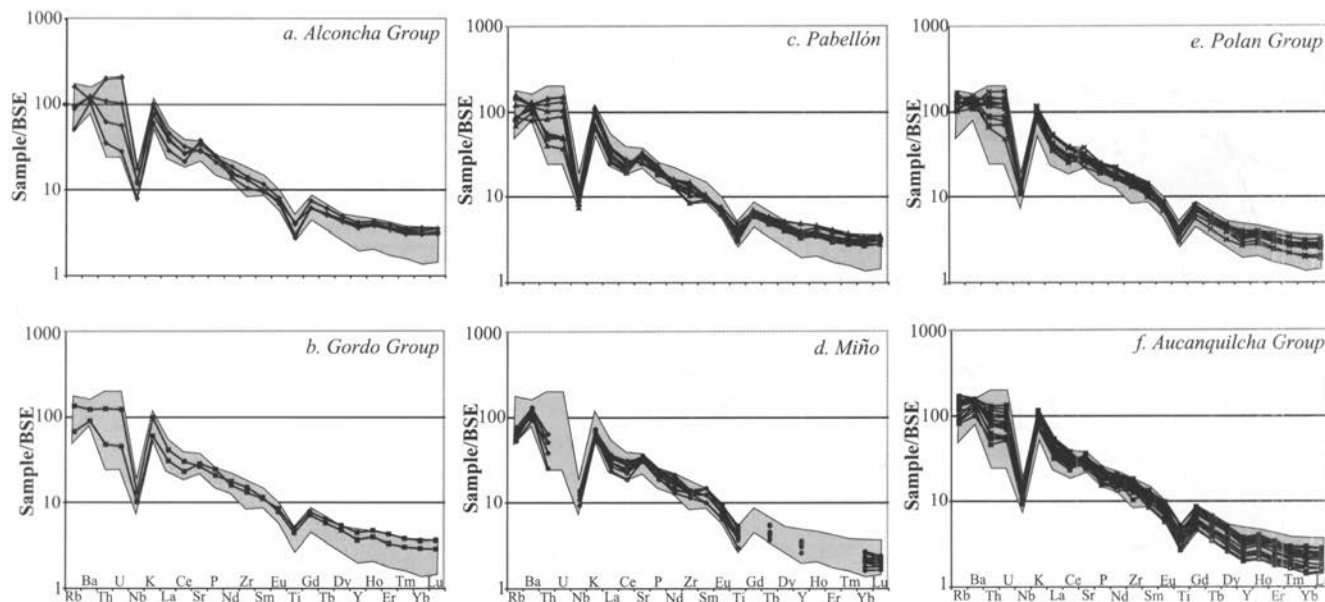
Figure 6 Trace element diagrams for eruptive groups at the AVC, broken out as in Figure 5. Shaded region represents full range of values for the AVC. BSE = bulk silicate earth values from McDonough & Sun (1995).

amphibole > orthopyroxene > clinopyroxene > biotite with rare occurrence of quartz and olivine with trace apatite and zircon. The amphibole occurs as two separate phenocryst populations, pargasite and hornblende, that occur in virtually all flows and the two varieties do not occur as overgrowths on one another (Klemetti & Grunder 2008).

3.8. Volume calculations: method and results

Footprint areas (A, Table 3) for volcanic edifices were obtained from the Ollagüe and Ujina 1:250 000 topographic maps with a base level of 3900 m. GIS treatment was not undertaken because digital elevation data of relevant scale were not available. Edifices were modelled as either simple cones, a frustum cone or as cylindrical lozenge (Table 3) or a combination of these. For cones, a radius (r and R) was calculated by taking the square root of area (A/π) and volume was calculated by using $1/3\pi r^2 h$, where h is the elevation difference from the break in slope and the summit. In cases of an extensive apron leading up to a cone, or for flat-topped edifices, the formulation of a frustrum cone (cone without peak) was used, that is, $1/3\pi h(R^2 + Rr + r^2)$, where R is the radius of the outer apron, and r is the radius at the break in slope for the main cone. For lava flow fields, a lozenge-shaped model was used; the area of the lava flow was multiplied by the average thickness, or height (Ah). All of these volumes are referred to as the 'Uncorrected volumes' (Table 3).

To correct for erosion, the relatively unglaciated stratocone, Volcán Miño (Fig. 2), was used as a model because it has only minor moraine development. The slope of Miño was calculated from the break in slope at 4500 m to the summit and has value of 0·55 m/m. Volumes for centres that exhibited effects from erosion and could reasonably be modelled as stratocones were recalculated by determining a new 'height' (h) using h = r*0·55, where r is the radius calculated from the footprint of the centre (Table 3). Domes such as Chaihuiri, Amincha or Inca were not corrected. This new height was then used to recalculate the volume using the cone equation and is referred to as the 'Corrected volumes' (Table 3). These corrected volumes were used to determine the cumulative volume curve and the rates of effusion.

Errors in the volume calculation derive from a number of factors: (1) uncertainty of footprint area; (2) uncertainty about

the original conical shape of the edifice; (3) underestimate or overestimate of the amount of glacial erosion; (4) underestimate of the volume of buried erupted material; and (5) loss of pyroclastic material to erosion or deposition away from the main complex. Volumes are likely to be accurate to within 5% for uncorrected domes and younger centres, while older centres that have been corrected are likely accurate to within 15%. Volumes for older centres may be skewed to values that are too low because of uncertainty of the extent of their footprints. The largest uncertainly is in the amount of older material potentially buried by the Aucanquilcha platform.

The pattern of early, compositionally diverse volcanism leading to a rapid increase in eruption rate and eruption of more homogeneous and more silicic magma is documented for other long-lived volcanic systems and implies a common development of the underlying magmatic system.

4. Discussion

4.1. Life span of the AVC

The arid climate of the Central Andes has preserved a record of at least 11 million years of volcanic activity at the Aucanquilcha Volcanic Cluster, as revealed by $^{40}Ar/^{39}Ar$ ages. Even the oldest known edifices, Cerro Alconcha and Volcán Tuco (formed at ~10–11 Ma) are recognisable as volcanic edifices. Whilst preservation may not allow identification of such long-lived systems in many settings, life spans on the order of several to ten million years have been established for a number of volcanic systems (Fig. 8). Long magmatic life spans are more commonly recognised in plutonic complexes. The long life span of the AVC invites the notion that it represents the volcanic sampling of a plutonic complex such as the Tuolumne Intrusive Suite (TIS), a continental arc plutonic complex of the Sierra Nevada Batholith. Like the AVC, the TIS was emplaced incrementally over ~10 million years in several magmatic episodes (Figs 7, 10).

4.2. Life-span of AVC volcanoes

Despite strategic sampling efforts, there are insufficient age data from individual volcanoes to confidently determine the life span of each centre, except for Volcán Aucanquilcha,

Table 2 Representative analyses of lavas and inclusions from the Aucanquilcha Volcanic Cluster.

Elements	AP-00-01 Alconcha	AP-00-04 Alconcha	AP-00-68 Amincha	AP-00-82 Amincha	AP2-00-46 Aucanquilcha	AP2-00-92 Aucanquilcha	AP2-00-71[i] Aucanquilcha	AP-00-76A Chaihuiri	AP-00-76C[i] Chaihuiri	AP-00-71 Gordo	AP-00-85 Gordo	AP-00-49 La Luna	AP-00-52 La Luna	VM99.12 Miño
Elements (wt.%)														
SiO_2	56·8	58·0	65·4	62·4	64·9	66·8	57·4	62·7	58·8	59·9	62·2	62·8	61·7	61·8
Al_2O_3	18·8	18·6	17·0	17·5	16·1	16·4	17·0	16·9	18·1	16·9	17·7	16·8	18·2	16·9
TiO_2	0·82	0·69	0·62	0·80	0·63	0·53	0·79	0·75	0·89	1·02	0·62	0·79	0·71	0·76
FeO*	6·19	6·70	4·48	5·01	3·75	3·11	5·86	4·53	5·75	5·76	4·43	4·49	4·53	5·25
MnO	0·12	0·14	0·07	0·10	0·06	0·05	0·09	0·08	0·09	0·09	0·08	0·07	0·07	0·09
CaO	7·20	6·87	4·67	5·30	4·00	3·47	7·12	4·86	6·14	5·50	5·11	4·81	4·79	5·50
MgO	3·86	3·29	1·66	1·69	1·93	1·49	2·87	2·52	3·34	3·4	2·50	2·56	2·43	3·04
K_2O	1·76	1·79	2·80	2·91	3·00	2·92	2·11	2·82	2·05	2·55	2·41	2·80	2·62	2·32
Na_2O	4·03	3·78	4·20	3·92	4·32	4·61	3·83	3·98	3·83	4·11	4·48	4·07	4·24	4·10
P_2O_5	0·25	0·25	0·19	0·24	0·18	0·16	0·15	0·21	0·23	0·30	0·21	0·21	0·24	0·23
Total	99·9	100·1	99·3	99·9	98·8	99·5	97·3	99·4	99·3	99·6	99·7	99·4	99·5	99·8
Elements (ppm)														
Ni	26	12	14	9	10	7	6	6	12	37	13	17	14	
Cr	41	15	17	13	25	12	23	28	36	130	5	44	43	
Sc	21	15	11	16	6	6	13	10	18	16	9	4	21	
V	182	141	108	109	82	71	140	121	166	136	115	114	125	
Ba	688	818	812	776	1009	1025	815	813	673	966	844	779	751	
Rb	31	35	116	95	87	81	56	71	49	67	62	7	78	
Sr	740	598	616	552	532	577	717	586	655	631	711	549	553	
Zr	116	123	153	148	154	148	119	151	135	193	143	153	142	
Y	14	18	18	17	12	9	13	16	16	22	11	14	20	
Nb	5·8	4·8	8·4	11·5	8·6	6·8	6·5	8·7	7·2	9·8	4·6	8·4	8·8	
Ga	22	18	19	18	23	22	19	21	20	21	20	22	21	
Cu	88	50	79	46	28	42	40	39	58	36	64	43	19	
Zn	80	78	67	82	74	64	90	78	94	103	69	82	75	
Pb	11	12	14	10	12	16	11	12	10	14	12	12	17	
La	24	33	31	33	24	21	41	44	26	36	15	17	19	
Ce	25	23	28	54	59	56	34	58	42	58	12	54	55	
Th	4	4	19	14	8	4	4	9	4	8	3	9	12	
Nd	17·3			23·2		18·2	21·6	22·9	19·0			21·5		
Sm	3·8			4·8		3·6	5·0	4·6	4·3			4·7		
Eu	1·1			1·2		0·9	1·3	1·1	1·2			1·2		
Gd	3·3			4·0		2·5	4·3	3·8	3·8			3·8		
Tb	0·5			0·6		0·3	0·6	0·5	0·6			0·6		
Yb	1·4			1·6		0·6	1·1	1·3	1·1			1·1		
Lu	0·2			0·2		0·1	0·2	0·2	0·2			0·2		
Ta	0·3			0·8		0·5	0·4	0·5	0·4			0·6		
U	0·6			4·1		1·5	1·0	1·8	1·1			2·5		
Sc	20·3	20·5	13·6	13·2	10·7	11·0	17·1	14·3	14·1			10·9		
V				11·9										

Table 2 *Continued.*

	VM99-52 Miño	AP2-00-01 Pabellón	AP-00-03 Pabellón	AP2-00-05¹ Pabellón	AP-00-37 Paco Paco	AP-00-38 Paco Paco	AP-00-08 Platform	AP-00-24 Platform	AP-00-61B¹ Platform	AP-00-73 Polan	AP-00-74 Polan	AP-00-89 Puquios	AP-00-94 Puquios	AP-00-64 Tres Monos	AP2-00-65 Tres Monos	AP-00-12 Tuco	AP-00-17 Tuco
Elements (wt.%)																	
SiO_2	65.0	62.8	61.0	55.7	61.9	59.1	62.4	62.1	55.7	62.6	61.2	58.7	57.4	61.4	63.2	61.6	62.7
Al_2O_3	17.0	16.2	17.0	18.9	16.7	16.9	16.3	19.3	18.0	17.3	17.7	17.9	17.7	16.4	17.0	17.8	18.0
TiO_2	0.57	0.70	0.75	0.94	0.85	0.95	0.80	0.42	1.10	0.71	0.83	0.94	0.96	0.88	0.70	0.59	0.56
FeO^*	3.99	4.80	5.39	6.51	4.89	6.03	4.68	3.17	6.97	4.88	5.31	5.87	6.40	5.18	4.44	4.58	4.65
MnO	0.06	0.09	0.10	0.11	0.08	0.09	0.08	0.06	0.10	0.08	0.07	0.10	0.12	0.09	0.07	0.10	0.10
CaO	4.54	4.81	5.54	7.39	5.07	6.06	4.73	5.78	7.39	4.85	5.56	6.63	7.09	5.20	4.86	5.26	5.24
MgO	2.19	2.74	3.26	4.10	2.81	3.58	2.68	2.22	3.91	2.68	2.52	2.75	4.26	3.15	2.49	2.23	2.35
K_2O	1.77	3.23	2.76	1.93	2.77	2.27	3.33	2.13	1.55	2.47	2.29	2.00	1.69	2.80	2.90	2.66	2.22
Na_2O	4.63	3.42	3.60	3.33	4.07	3.96	3.82	4.79	3.70	4.16	4.26	4.26	3.99	3.95	4.22	4.01	4.15
P_2O_5	0.20	0.19	0.18	0.22	0.21	0.26	0.24	0.15	0.25	0.19	0.23	0.26	0.24	0.25	0.20	0.25	0.21
Total	96.4	99.0	99.6	99.1	99.4	99.2	99.1	100.2	98.7	100.0	100.0	99.4	99.8	99.3	100.1	99.1	100.1
Elements (ppm)																	
Ni		23	23	17	17	22	14	14	19	16	19	14	41	20	14	4	14
Cr		54	28	26	44	82	49	18	33	28	26	17	83	66	29	3	19
Sc		14	12	16	8	18	10	9	16	13	12	12	18	16	6	16	7
V		125	156	212	137	160	115	51	174	124	125	152	172	133	117	151	88
Ba		743	694	673	807	763	879	867	610	796	748	690	599	928	812	655	807
Rb		88	74	40	80	55	91	39	35	68	60	47	41	74	79	31	52
Sr		468	504	618	521	620	579	758	609	554	586	565	550	635	572	694	568
Zr		162	141	114	161	158	171	109	134	143	144	154	139	180	154	116	139
Y		18	16	18	15	16	13	13	17	10	15	20	18	17	14	17	15
Nb		8.1	7.1	6.3	8.8	8.7	9.6	5.2	7.2	6.9	7.7	7.2	8.5	8.8	8.2	5.8	8.0
Ga		19	18	20	21	22	18	24	22	17	22	19	18	21	20	19	19
Cu		32	32	22	30	45	35	37	83	44	49	62	32	42	49	79	45
Zn		69	71	77	79	96	86	67	101	74	84	89	86	90	74	75	68
Pb		12	11	9	10	17	14	11	20	12	12	10	7	13	13	10	8
La		17	17	16	47	32	32	26	21	2	23	25	34	40	26	20	18
Ce		48	57	15	51	62	61	40	47	21	61	42	48	79	50	31	40
Th		8	10	4	7	8	12	7	4	10	6	5	2	10	11	5	6
Nd				16.4	21.7		26.0				20.4		19.4	27.8	20.8	20.0	19.0
Sm				3.9	4.6		5.1				4.5		4.4	5.5	4.2	4.1	4.1
Eu				1.2	1.2		1.2				1.2		1.3	1.3	1.1	1.1	1.1
Gd				3.5	3.7		3.9				3.8		4.1	4.3	3.3	3.3	3.3
Tb				0.6	0.6		0.5				0.5		0.6	0.6	0.5	0.5	0.5
Dy															2.6	2.9	3.0
Yb				1.5	1.3		1.1				1.3		1.5	1.2	1.1	1.4	1.5
Lu				0.2	0.2		0.2				0.2		0.2	0.2	0.2	0.2	0.2
Ta				0.3	0.6		0.7				0.5		0.4	0.6	0.6	0.6	0.7
U				0.7	2.4		2.8				1.8		0.9	2.2	2.5	1.1	2.0
Sc				20.0	12.9		12.2				14.3		20.5	13.6	11.9	10.7	11.0

Representative analyses for lavas and inclusions from the Aucanquilcha Volcanic Cluster derived from XRF, ICP-MS and INAA (see text for methods).
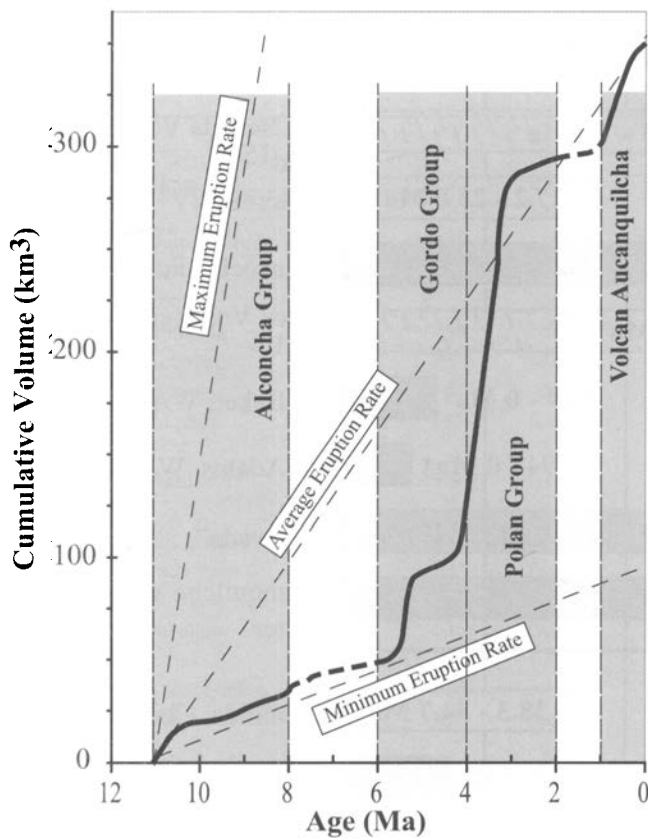¹Indicates sample is magmatic inclusion.

Figure 7 Cumulative volume versus age plot for the AVC. Dark line represents the cumulative volume erupted in the AVC based on field mapping and $^{40}Ar/^{39}Ar$ geochronology. Grey shaded areas bounded by dashed lines represent the eruptive groups. Light regions were the cumulative volume line is dashed are possible hiatuses in volcanic activity in the cluster. Light dashed lines represent the extrapolated maximum, minimum and average eruption rates at the AVC. Maximum and minimum rates serve to illustrate how the choice of time interval can drastically affect the estimated volcanic output rate.

which has been building for at least 1 m.y. and is potentially active Now-extinct Volcán Miño is similarly long-lived. Ranges of dates for other multiple-dated centres indicate life spans of 0.5 ± 0.1 m.y. (Tuco, Alconcha, Gordo, Puquíos, Polan, La Luna, and Tres Monos). When the 2 σ error is taken into account, the range in the age data for each of these edifices varies from analytically indistinguishable to 0·9–1·3 m.y. These are minimum ranges, inasmuch as older parts of the edifices may not be exposed or may have been missed in sampling. On the Altiplano, lack of dissection is the main limitation to sampling.

The volcanoes Paco Paco and Pabellón appear shorter lived, with life spans of 0·25 m.y. to 0·3 m.y. Considering analytical error, they may have lasted as long as 0·6 m.y. and 0·75 m.y. respectively. Despite the sampling limitations, the similarity in age range for most of the edifices indicates that there is a typical time-span over which magmatic plumbing delivers material to feed a single volcanic edifice, and that for most of the AVC it is about 0·5 m.y. to 1 m.y., comparable to other large, subduction-related composite centres (Fig. 8) and to some discrete arc plutonic complexes, such as the Yerington Batholith (Dilles & Wright 1988).

4.3. Eruptive volumes and rates at the Aucanquilcha Volcanic Cluster

The Aucanquilcha Volcanic Cluster has erupted 327 ± 20 km^3 (erosion-corrected) of magma (DRE) over the past 11 million years (Table 3). The largest extant edifice is Volcán Aucan-

quilcha, with a volume of ~37 km^3. At least three other edifices have volumes of ≥ 30 km^3: Gordo, Polan-La Luna and Tres Monos. Two edifices, Miño and Alconcha, are ≥ 10 km^3. These data, coupled with age ranges, are used to arrive at volcanic output rates, bearing in mind that such rates are highly skewed by the age range over which volumes are integrated. For example, the volcanic output rate for Volcán Aucanquilcha has an average of 0·04 km^3/k.y., but varies from 0·16 km^3/k.y. in early stages to 0·01 km^3/k.y. in more recent time (Klemetti & Grunder 2008). Similarly, the average volcanic output rate at the AVC has been ~0·03 km^3/k.y. over 11 m.y., but varies substantially during that time.

The three early stages of activity of the AVC range about 2 m.y. in duration (Figs 3, 7) and the present phase, Volcán Aucanquilcha, has persisted 1 m.y. The Alconcha Group (11–8 Ma) erupted a total volume of 46 km^3, resulting in an average rate of ~0·013 km^3/k.y. (Table 4; Fig. 7). Following a ~2 million year hiatus (Fig. 3), the Gordo Group added 55 km^3 yielding a rate of 0·027 km^3/k.y. over 1·7 million years (Figs 3, 7). The hiatus in volcanism between the Alconcha and Gordo Group is bracketed by Cerro Amincha at ~8 Ma and Cerro Puquíos at ~5·8 Ma. The hiatus in activity may be a sampling artefact, if vents of these first two groups are obscured beneath ejecta of younger volcanoes.

The eruptive rate increased sharply with onset of the Polan Group. During these 1·9 million years, at least 154 km^3 of lava were erupted at an average rate of 0·077 km^3/k.y., a rate almost one and a half times greater than any other eruptive stages in the AVC (Figs 7, 9). Even if it is assumed that as much as a third of the volume of the Aucanquilcha Platform should be assigned to older, covered volcanic groups, this reassignment would not substantially affect the volume increase during the Polan Group activity (Fig. 7). Following the Polan Group, the eruption rate slowed, with eruption of Volcán Aucanquilcha to 0·04 km^3/k.y.

The overall rate of volcanic output of the AVC, 0·03 km^3/k.y., is ten to 100 times less than most silicic volcanic output estimates compiled by White et al. 2006 and three to ten times less than for the CVZ overall. The volcanic output rate of the CVZ is estimated at 0·11 km^3/k.y. over the past 28 m.y. (Baker & Francis 1978) and about 0·37 km^3/k.y. over the past 10 m.y. (Francis & Hawkesworth 1994). The lower volcanic output rate at the AVC likely reflects local versus regional output rates and is perhaps related to the AVC lying at the edge of the voluminous and ignimbrite-dominated Altiplano–Puna Volcanic Complex.

4.4. Evolution of the AVC and comparison to other long-lived volcanic complexes

Early phases of the AVC were a period of relatively low volcanic output rate and compositionally diverse volcanism. During eruption of the Alconcha and Gordo Group the most mafic lavas were erupted and mafic silicate mineral assemblages were largely anhydrous (pyroxene ± olivine). This period of incubation lasted approximately six million years, after which volcanic output rate increased sharply, and volcanism became more silicic and homogenous, with most lavas having 62 to 64 wt.% SiO$_2$ and amphibole ± biotite. This trend is interpreted to reflect the development of a substantial dacitic magma reservoir beneath the core of the AVC, where the thermal memory of preceding widespread magma passage would be greatest. The development of an integrated silicic magma reservoir, or mush zone, is supported by the observation that more mafic, andesitic magmas occur commonly as lavas prior to Polan time and mainly as mafic inclusions thereafter. A silicic magma reservoir would provide a density barrier to the passage of denser magma. At Cerro Pabellón,
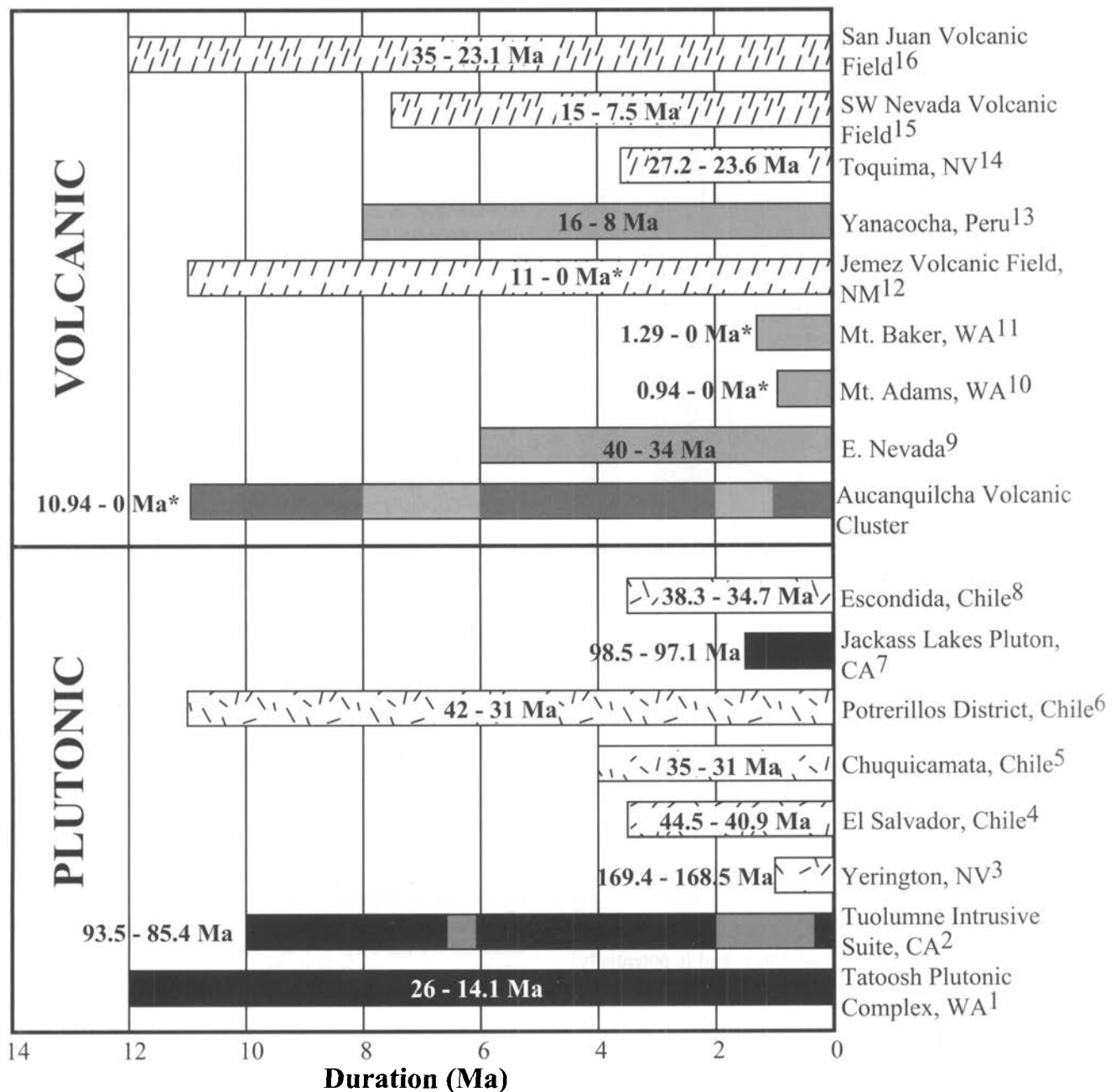
Figure 8 Longevity of major plutonic and volcanic magmatic systems compiled for comparison to the AVC with published age range for each. The AVC and the TIS are divided into periods of activity (dark) and hiatuses (light). * indicates that system is still potentially active. Among volcanic systems, diagonal dashes indicates those with significant ignimbrites and the plain pattern indicates systems where lavas are dominant. Among plutonic systems the speckled pattern indicates those associated with porphyry copper deposits.
Data compiled from the following sources: [1]Mattinson 1977; [2]Coleman *et al.* 2004; [3]Dilles & Wright 1988; [4]Gustafson *et al.* 2001; [5]Ballard *et al.* 2001 (with precursor activity of at least 5 m.y.); [6]Marsh *et al.* 1997; [7]McNulty *et al.* 1996; [8]Richards *et al.* 2001; [9]Grunder 1995; [10]Hildreth & Lanphere 1994; [11]Hildreth *et al.* 2003; [12]Gardner *et al.* 1986; [13]Longo 2005; [14]Boden 1986; [15]Sawyer *et al.* 1994; [16]Lipman 2000.

andesite occurs as lavas and as quenched inclusions, indicating the onset of a substantial low-density, dacite magma reservoir at ~4 Ma (Figs 9, 10). Volcán Miño erupted abundant andesite lavas during the time of increased volcanic output. The present authors interpret that its peripheral position on the western edge of the AVC lies outside the dacitic reservoir of Polan time. They infer the depth of the integrated dacitic (granodioritic) magma reservoir to be in the middle to upper crust where hydrous silicates are available to facilitate melting and consistent with the palaeodepth of many granitoid batholiths based on contact aureole systematics (Barton *et al.* 1991).

Volcán Aucanquilcha represents a time of decreased volcanic output and evolution to a still more central and more

silicic magma reservoir compared to Polan time activity; Aucanquilcha lavas have mainly 64–66 wt.% SiO_2, ubiquitous amphibole and abundant biotite. Inclusions from Aucanquilcha have higher average silica (59–60 wt.%) than inclusions of earlier groups (typically <59 wt.%), indicating increased density filtering with increased degree of differentiation of the magmatic system (Fig. 10). Amphibole data from Volcán Aucanquilcha are consistent with palaeodepths of 6 to 10 km for the most evolved dacitic part of the magma reservoir (Klemetti 2005).

This pattern of protracted diverse volcanism followed by a burst of silicic volcanism is not unique to the AVC. The same evolution is seen at the Yanacocha Volcanic Complex, Perú in

Table 3   Areas, heights and volumes for the Aucanquilcha Volcanic Cluster.

Centre	Age (Ma)	Model	Area (km^2)	Height (km)	Uncorrected volume (km^3)	Corrected volume (km^3)
Tuco	11	dome	4·7	0·2	0·3	1·1
Alconcha	10·5	frustum	28·5	0·5	10·8	15·7
		dome	11·4	0·3		
Ujina Ignimbrite	9·4[b]	c	n/a	n/a	4·5	4·5
Coscalito	8·8[b]	dome	29·7	0·6	5·9	5·9
Coasa	8[b]	dome	35·2	0·7	8·2	8·2
Amincha	7·99	dome	27·7	0·5	4·6	4·6
Achupella	7·5[b]	dome	18·9	0·4	2·5	2·5
Inca	7·5[b]	dome	23·5	0·5	3·9	3·9
Puquíos	5·6	frustum	16·4	0·2	3·6	6·8
		dome	7·5	0·5		
Gordo	5·5	frustum	53	0·8	30·3	36·9
		dome	15·5	0·85		
Las Bolitas	5·3	cylinder	54·6	0·1	5·5	5·5
Paco Paco	4·3	frustum	14·1	0·4	3·8	5·5
		dome	3·3	0·5		
Pabellon	4·1	frustum	18·7	0·6	8·6	9·4
		dome	6·5	0·6		
Aucanquilcha Platform	3·55	cylinder	300	0·9	100	100
Miño	3·3	frustum	45·3	0·35	14·5	14·5
		dome	12·2	1·25		
Polan	3·3	frustum	39·1	0·6	12·5	12·5
		dome	4·5	0·75		
Pampas[a]	3·3	lozenge	43·7	0·02	0·9	0·9
La Luna[a]	3·3	frustum	42·2	0·8	18·7	18·7
		dome	7·8	0·2		
Casisca Flow[a]	3·3	lozenge	26·5	0·02	0·5	0·5
Tres Monos	3·0	frustum	87·7	0·55	29·2	29·2
		dome	17·3	0·50		
Chaihuiri	2·3	dome	13·3	0·7	3·1	3·1
Aucanquilcha	0·9	dome	37	1·5	37	37
TOTAL AVC					308·9	326·9

Volumes calculated for centres in the Aucanquilcha Volcanic Cluster. Edifices older than Volcán Miño are corrected for erosion with Miño as a model (see text for full description of the erosion correction used).
[a]Indicates subcentres of Cerro Polan. All ages are from this study unless noted.
[b]Ramirez & Huete (1981).
[c]Indicates that the volume is take from deSilva & Francis (1991).

Table 4   Eruption rates for the volcanic groups at the Aucanquilcha Volcanic Cluster.

Group	No. of centres	Vol. (km^3)	Time span (Ma)	Rate (km^3/ky)
Alconcha	7	46	3	0·013
Gordo	~4	55	2	0·027
Pabellon	1	9	a	a
Miño	1	14·5	a	a
Polán	~5	154[b]	2	0·077
Aucanquilcha	1	37	1	0·040
TOTAL AVC	~19	325	11	0·030

Summary of the calculated rates of eruption for the stages of volcanism at the Aucanquilcha Volcanic Cluster. a=Indicates no rate calculated for single centre as the volumes for Volcán Miño and Volcán Pabellón are included in the calculation for the overall rate of the Polan Group. [b]Indicates that the volume includes all lavas of the Aucanquilcha Platform (~100 km^3).

mid-Tertiary volcanic rocks of eastern Nevada, and at the San Juan Volcanic Complex (Fig. 9). All have life spans similar to the AVC and are intermediate to silicic continental volcanic suites; most have some associated ignimbrite activity. Similar to the AVC, the early volcanic history for these systems is one of compositional diversity distributed over a broad area, which after several million years of activity results in a rapid increase in eruption rate and a change to dominantly silicic (dacite and rhyolite) volcanic rocks bearing amphibole and biotite and which are distributed over a smaller, more central region. In the Yanacocha system amphibole is nearly ubiquitous, but increases and is joined by biotite with the onset of voluminous dacitic volcanism. Despite a gross similarity in development amongst these volcanic fields, they differ vastly in volume, ranging from cumulative volumes of 10^0 to 10^4 km^3. On the other hand, the average thickness of volcanic cover (DRE) is similar; values range from 0·2 km at Yanacocha to 0·7 km (eastern Nevada) with the AVC and the San Juan Volcanic Field at ~0·5 km.

In the case of the AVC and Yanacocha, the onset of pervasive hydrothermal alteration can be constrained to co-incide with the rapid production of biotite dacite (Fig. 9). For the AVC, the ages of alteration are constrained by dating of unaltered lavas that cap alteration. For Yanacocha, Longo (2005) has dated alunite as well as fresh volcanic rocks. The present authors infer that the creation of an integrated central
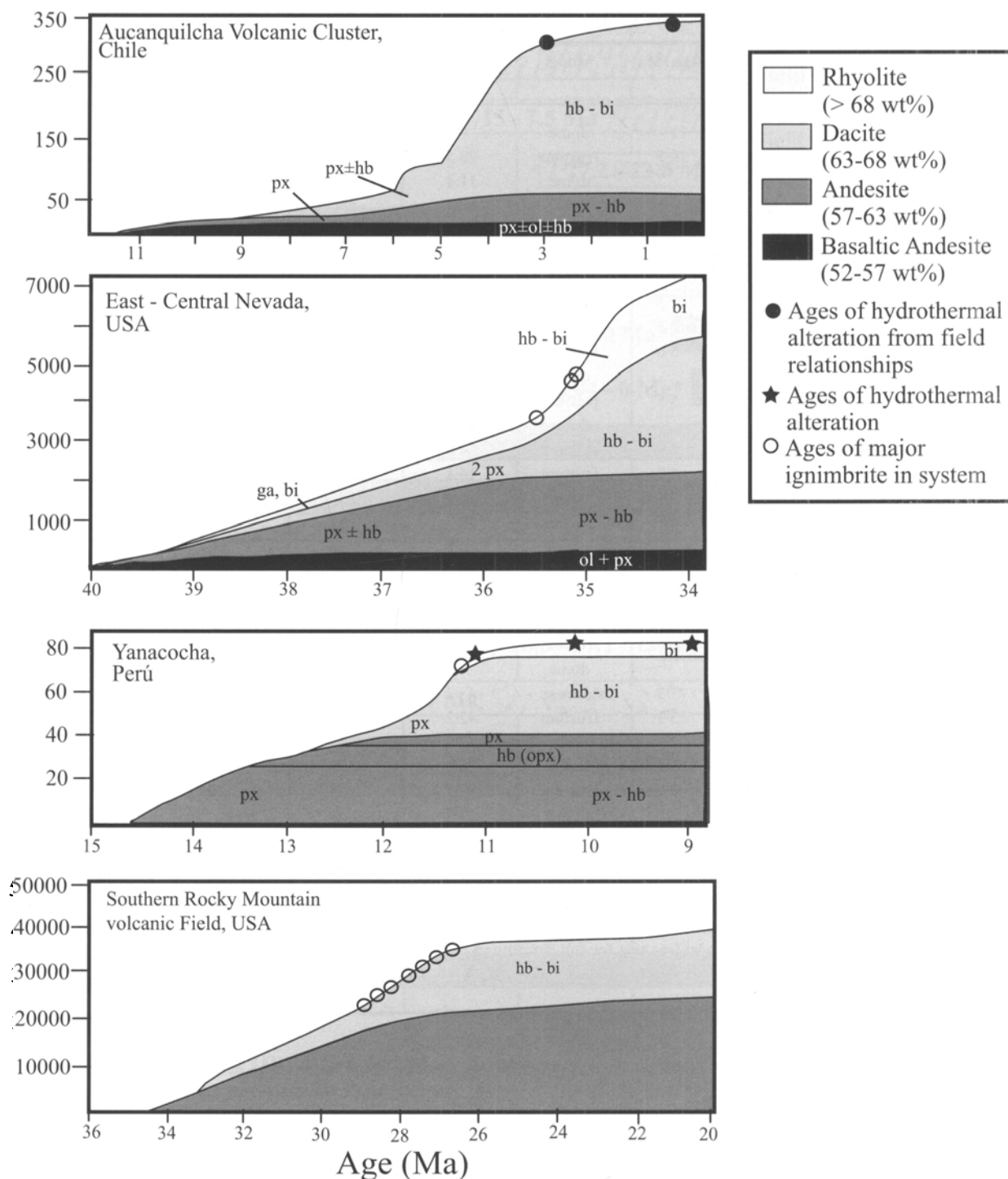
Figure 9 Schematic plots illustrating the life span, cumulative volume, bulk composition and mineralogical development of the AVC, Tertiary volcanic rocks of eastern Nevada (Gans *et al.* 1989; Grunder 1995), for Yanacocha, Perú (Longo 2005), and for the San Juan Volcanic Field (Lipman 2007).

Figure 10 Cartoon illustrating potential evolution of the AVC in the Andean crust based on the development of the AVC in four stages. Stippled pattern represents the upper 55 km of continental crust in the central Andes of northern Chile. The shading represents the same magmatic compositions as found in Figure 9; lighter colours reflect higher silica. Areas with outline and light grey pattern represent the intrusions from the previous stages of magmatism. Small circles signify the entrainment of magmatic inclusions. The white-grey box in the right-most panel (Aucanquilcha) represents the area of crust reworked by repeated heating from the intrusion of magma. On the surface profile (not to scale), active systems are black and inactive systems are grey. The overall development is of fitful intrusion and extrusion of compositionally diverse magma, derived from more mafic magmas stalled in a MASH-like zone (Hildreth & Moorbath 1988) or hot zone (Annen *et al.* 2006) in the deep crust – shown schematically as crosses at the base. By the time of the Polan Group, an integrated magma reservoir was trapping subjacent andesite and hydrothermal convection had initiated. The two-stage reservoir at Aucanquilcha time is consistent with two populations of amphibole and amphibole barometry (Klemetti 2005).
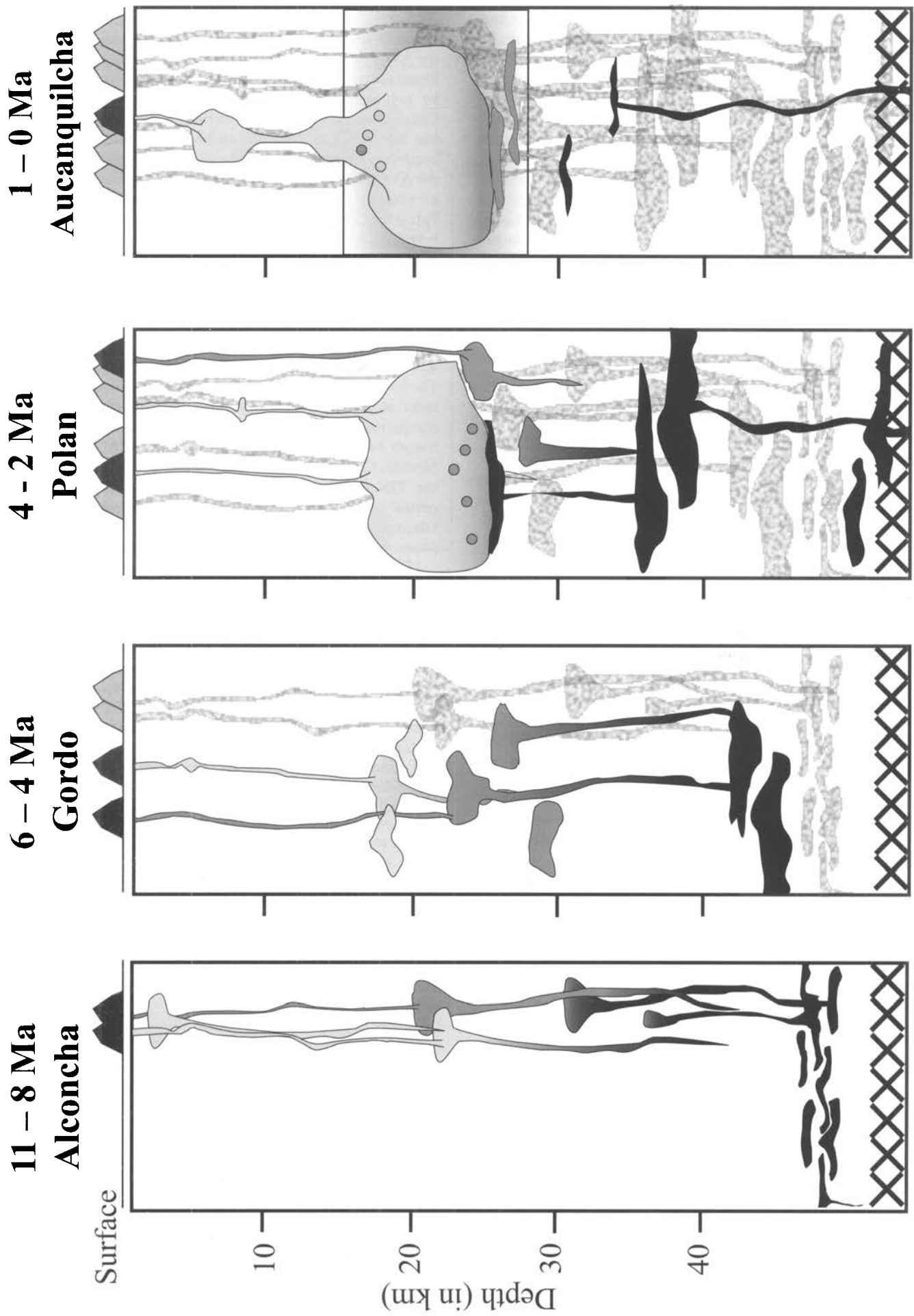
silicic magma reservoir is related to driving hydrothermal circulation. Cu-porphyry deposits, which are common in the Central Andes, are linked with multiple intrusions of granitoid magmas in continental settings. Many of these porphyry systems have life spans of a few million years (Fig. 8), and might be seen as the plutonic equivalent of the later Polan and Aucanquilcha phases of the AVC.

The timing of major ignimbrite volcanism is also consistent with development of a large silicic magma reservoir after a period of magmatic incubation. In the case of eastern Nevada, regional ignimbrites (the Kalamazoo Tuff and Tuff of North Creek at 35 Ma and the Tuff of Cooper Summit at 35·7 Ma; Gans *et al.* 1989) occur with the burst in biotite dacite volcanism. Ignimbrites that are part of the Yanacocha Volcanic Complex occur as part of the dacitic burst (San Jose Ignimbrite, 11·2–11·5 Ma; Longo 2005). In the San Juan Volcanic Field, the most voluminous ignimbrite activity, including the Fish Canyon Tuff, defines the dacite pulse.

What causes the sudden onset of hornblende biotite dacite and sudden increase in eruption rate? The increased eruption rate may reflect increased magma supply, in turn driven either by increased supply of magma from the mantle, or by thermal feedback in the central part of the magma complex, or indeed both. Very similar time-volume evolution of the Altiplano–Puna Volcanic Complex, a vast volcanic field at the scale of the San Juan Volcanic Field, suggests that the underlying cause is at a vast scale and likely driven by influx of mantle-derived basalts (de Silva & Gosnold 2007). On the other hand, isotopic signatures of silicic continental suites indicate substantial crustal feedback. Crustal modulation of thermal input via magmas is also indicated by the centralisation of magmatism, such as at the AVC. By crustal feedback we mean a balance between heating of the crust by injection and crystallisation of magma and heat loss by cooling and by reaction of magma with the crust (melting, assimilation, dissolution).

An additional factor in creating a pulse of dacitic volcanism is that storage of more magma at shallower depths would facilitate eruption, as suggested by de Silva (1989), consistent with the timing of ignimbrites and hydrothermal alteration with increased volcanic output rate. The evolution to biotite hornblende dacite suggests a general cooling and possible addition of water through assimilation of altered wallrocks, and (or) crystallisation, consistent with more shallow, cooler conditions of upper reaches of the magmatic system.

Whatever the cause, the pattern of sharp increase in eruption rate of silicic magma after a period of more compositionally diverse volcanism is pronounced in a range of volcanic systems. Whilst modest volcanism and hydrothermal alteration may persist after the volumetric climax for a few million years, it appears that the system soon wanes and eventually dies. This suggests that the AVC is in its waning stage.

4.5. Temporal and spatial distribution of volcanism
The geographic distribution of volcanic vents in the AVC (Fig. 2) indicates a change in the distribution of volcanism from peripheral (or widespread) to more centralised with time. Within this general pattern there are linear arrays of vents. The most prominent array is the east-west alignment of the six volcanic vents that make up Volcán Aucanquilcha. Projection of this array to the west includes the La Luna and Cerro Polan centres, suggesting the existence of a conduit system focused on an east-west crustal fissure or weakness, as old as ~2·6 m.y., and along which the main hydrothermal activity of the AVC has been focused. Besides the general trench-parallel trend of the volcanic arc, east-west alignment of vents is the most common lineament among young volcanoes in the region

and likely reflects a regional stress field (Klemetti & Grunder 2008).

North-south alignments occur in the northeast quadrant of the AVC, east of 68°30'W and north of Aucanquilcha (Fig. 2). These are defined by the north-south ridge of Tres Monos and by two *en echelon* alignments of the northeastern domes, Coasa-Coscalito and Achupella–Inca–Amincha. Dikes on the east side of Volcán Tuco also strike north-south. A more vague northwest alignment of vents occurs in the western portions of the AVC (west of 68°30'W). The vents of Volcán Tuco fall on a ~N40W trend with Cerro Alconcha and the edifices of Pabellón, Cerro Negro, Cerro Puquíos, Cerro Gordo define a ~N50W trend. Overall, the AVC appears to mimic the finding of Mathieu *et al.* (2008) who suggest that peripheral to central vent distribution along fractures, expressed as vent alignments, reflects failure of the upper crust in response to broad doming caused by progressive intrusion at depth.

4.6. Comparison to the Tuolumne Intrusive Suite
The long life span and the eruptive history indicating development of an integrated magma reservoir at depth invite the comparison of the AVC to plutonic suites. We draw on the history of the Tuolumne Intrusive Suite (TIS) in the Sierra Nevada, California (Fig. 11). Similarity between the AVC and the TIS includes general development from peripheral to central magmatism (Kistler & Fleck 1994; Coleman *et al.* 2004; Glazner *et al.* 2004; Fig. 11) with zonation from more mafic phases on the margin to more silicic compositions in the centre.

U-Pb geochronology for the Cretaceous TIS suite indicates fitful assembly over a period of ~10 m.y. (95–85 Ma) (Coleman *et al.* 2004). Ages decrease toward the centre of this normally zoned batholith that is composed of at least five plutons (Kistler *et al.* 1986), marking several intervals of magmatic activity (Fig. 11). The dominant pulse includes the Half Dome Granodiorite and the Cathedral Peak Granodiorite. These represent most of the outcrop area (Fig. 11). The comparison to the AVC is striking in that the most voluminous plutonic phase is broadly distributed in the centre of the TIS and occurs after several million years of magmatism, similar to the Polan Group pulse. The youngest pluton, the Johnson Granite, crops out in the centre, analogous to Volcán Aucanquilcha in the centre of the AVC (Fig. 11).

The footprint of the TIS is two to three times that of the AVC. The number of volcanoes in the AVC exceeds the number of plutons in the TIS. This suggests that plutons may feed several volcanoes, consistent with episodes of plutonic magmatic activity lasting a few hundred thousand to a million years, probably as intermittent thermally rejuvenated crystal mush complexes. Such a history for the TIS is supported by evidence for zircon growth and recycling in the TIS (Miller *et al.* 2007).

5. Conclusions
The nineteen volcanoes of the Aucanquilcha Volcanic Cluster (AVC), ~21°15'S in Chile, document at least 11 million years of arc volcanism in the Central Andes and provide one of the longest records of virtually continuous magmatism in a continental volcanic complex. Volcanic edifices of the AVC typically have age ranges of 0·5 m.y. to about 1 m.y. and are mainly made of lavas. Stages of volcanic activity in the AVC each last 1·5 m.y. to 3 m.y. and produce six or more volcanoes: the Alconcha Group (~11 Ma to 8 Ma), the Gordo Group (~6 Ma to 4 Ma), and the Polan Group (4 Ma to ~2 Ma). The present stage is the construction of Volcán Aucanquilcha in the centre of the AVC, since ~1 Ma. Rocks of these
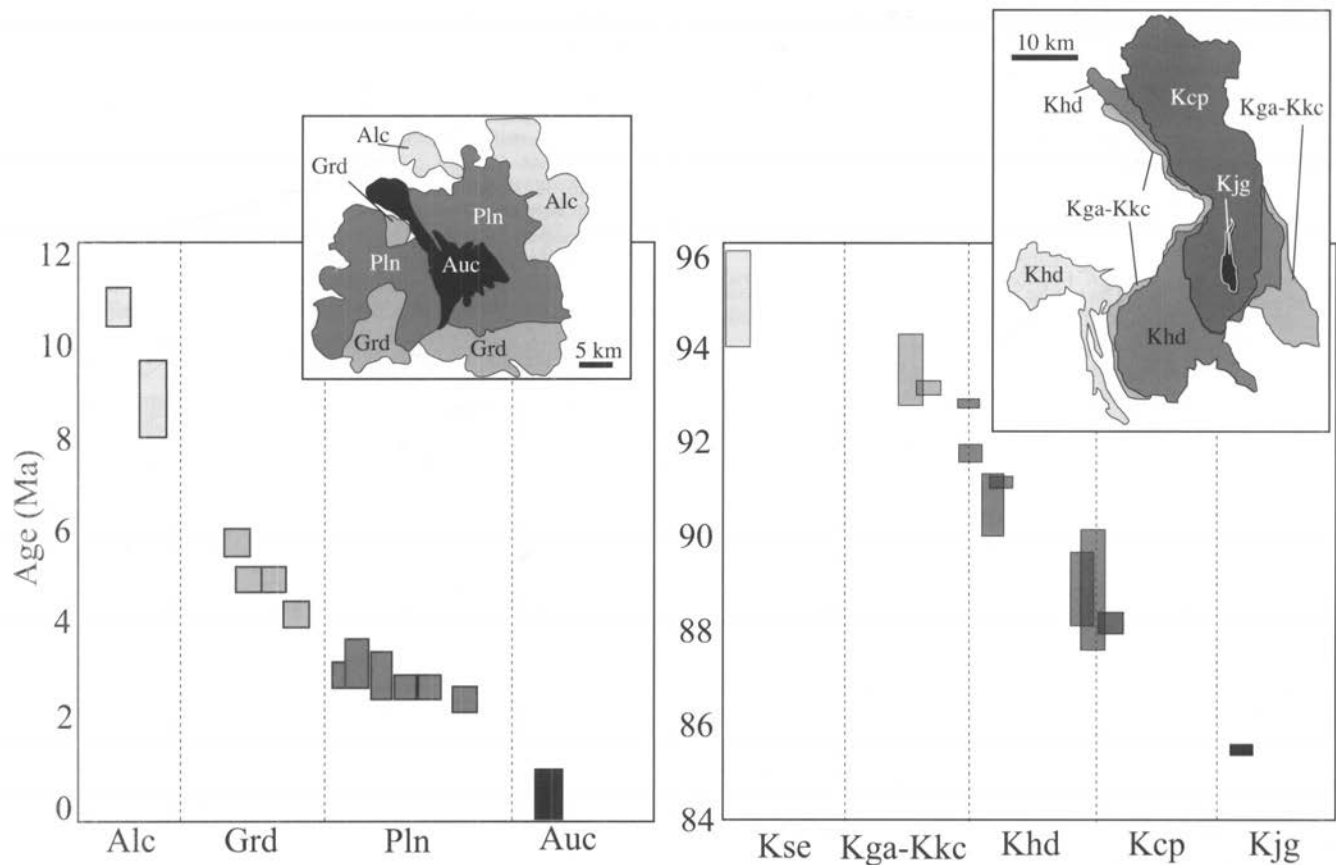
Figure 11 Temporal Distribution of magmatism in the Tuolumne Intrusive Suite and the AVC: (A) The footprint and age vs. unit distribution of the Tuolumne Intrusive Suite (TIS) based on U-Pb concordant zircon. Stratigraphic units for the TIS are: (Kse) Sentinel Granodiorite; (Kga-Kkc) Glen Aulin-Kuna Crest Granodiorite; (Khd) Half Dome Granite; (Kcp) Cathedral Peak Granodiorite; (Kjg) Johnson Granite. Taken from Glazner *et al.* (2004). (B) The footprint and age versus unit distribution of the AVC from K-Ar and Ar-Ar age data for AVC (right), shown at approximately the same scale. Abbreviations: (Alc) Alconcha Group; (Gordo) Gordo Group; (Polan) Polan Group; (Aucan) Volcán Aucanquilcha.

successive groups describe (1) a pattern of activity in the AVC from peripheral to central; (2) a corresponding change from compositionally diverse, crudely bimodal, andesite-dacite volcanism to more homogenous and increasingly silicic; (3) a change from early anhydrous mafic silicate assemblages (pyroxene dominant) to later biotite amphibole dacite; (4) an abrupt increase in eruption rate associated with voluminous biotite dacite; and (5) the onset of pervasive hydrothermal alteration. Virtually identical overall evolutionary patterns exist among other long-lived continental volcanic suites (Gans *et al.*1989; Grunder 1995; Longo 2005; Lipman 2007).

The long time scale and broadly granitoid bulk composition of the AVC suggests that it is the volcanic analogue of a batholith assembled over a period of ~11 m.y. in successive plutonic pulses that leave a normally-zoned intrusive complex. After several million years of fitful activity, a unified granodioritic mush, capable of repeatedly erupting dacite, is assembled and acts as a density filter to more mafic magmas. The development of a substantial, unified magma reservoir in the AVC is indicated by (1) a pulse of dacitic volcanism and centralisation of vent distribution; (2) the restriction of late andesite to occurrence as magmatic inclusions, implying density trapping of more mafic magmas; (3) the occurrence of extensive hydrothermal alteration, implying a substantial magmatic heat source at moderate depth; and (4) seismic attenuation (Haberland & Rietbrock 2001) and high electrical conductivity (Schwarz & Krüger 1997) in the middle to upper crust. The Cretaceous Tuolumne Intrusive Suite of the Sierra Nevada, California, provides a likely batholithic analogue, in

that it shares a similar ~10-m.y. life cycle and is composed of a succession of shorter-lived granitoid (diorite to granodiorite to granite) plutons arranged from peripheral to central in time, with the largest plutonic unit occurring after ~5 m.y. of magmatic incubation, and with the most evolved unit last and central.

6. Acknowledgements

7. References

Annen, C., Blundy, J. D. & Sparks, R. S. J. 2006. The genesis of intermediate and silicic magmas in deep crustal hot zones. *Journal of Petrology* 47 (3), 505–39.

Bacon, C. R., Persing, H. M., Wooden, J. L. & Ireland, T. R. 2000. Late Pleistocene granodiorite beneath Crater Lake caldera, Oregon dated by ion microprobe. *Geology* 28 (5), 467–70.

Baker, M. C. W. 1977. *Geochronology and volcanology of Upper Cenozoic volcanic activity in north Chile and south-west Bolivia.* Ph.D. Dissertation, The Open University, UK.

Baker, M. C. W. 1981. The nature and distribution of upper Cenozoic ignimbrite centres in the Central Andes. *Journal of Volcanology and Geothermal Research* 11 (2–4), 293–315.

Baker, M. C. W. & Francis, P. W. 1978. Upper Cenozoic volcanism in the central Andes; ages and volumes. *Earth and Planetary Science Letters* 41 (2), 175–87.

Ballard, J. R., Palin, J. M., Williams, I. S. & Campbell, I. H. 2001. Two ages of porphyry intrusion resolved for the super-giant Chuquicamata copper deposit of northern Chile by ELA-ICP-MS and SHRIMP. *Geology* 29 (5), 383–6.

Barton, M. D., Staude, J.-M., Snow, E. A. & Johnson, D. A. 1991. Aureole Systematics, *In* Kerrick, D. M. (ed.) *Contact Metamorphism. Reviews in Mineralogy* 26, 723–847.

Boden, D. R. 1986. Eruptive history and structural development of the Toquima caldera complex, central Nevada. *Geological Society of America Bulletin* 97, 61–74.

Chmielowski, J., Zandt. G. & Haberlan, C. 1999. The Central Andean Altiplano–Puna magma body. *Geophysical Research Letters* 26, 783–6.

Clark, A. H. 1970. An occurrence of the assemblage, native sulfure-covellite-'Cu5.5FexS6.5x', Aucanquilcha, Chile. *American Mineralogist* 55, 913–18.

Coleman, D. S, Gray, W. & Glazner, A. F. 2004. Rethinking the emplacement and evolution of zoned plutons: Geochronologic evidence for incremental assembly of the Tuolumne Intrusive Suite, California. *Geology* 32, 433–6.

Cooper, K. M., Reid, M. R., Murrell, M. T. & Clague, D. A. 2001. Crystal and magma residence at Kilauea Volcano, Hawaii: 230Th-226Ra dating of the 1955 east rift eruption. *Earth and Planetary Science Letters* 184, 703–18.

Costa, F. & Singer, B. 2002. Evolution of Holocene dacite and compositionally zoned magma, Volcán San Pedro, Southern Volcanic Zone, Chile. *Journal of Petrology* 43 (8), 1571–93.

Crock, J. G. & Lichte, F. E. 1982. Determination of rare earth elements in geological materials by inductively coupled argon plasma atomic emission spectrometry. *Analytical Chemistry* 54 (8), 1329–32.

Davidson, J. P., McMillan, N. J., Moorbath, S., Worner, G., Harmon, R. S. & Lopez-Escobar, L. 1990. The Nevados de Payachata volcanic region (18S/69W, N. Chile): II. Evidence for widespread crustal involvement in Andean magmatism. *Contributions to Mineralogy and Petrology* 105, 412–32.

Davidson, J. P., Harmon, R. S. & Worner, G. 1991. The source of central Andean magmas; Some considerations. *In* Harmon, R. S. & Rapela, C. W. (eds) *Andean magmatism and its tectonic setting*, 233–43. Boulder, CO: Geological Society of America.

Deruelle, B., Harmon, R. S. & Moorbath, S. 1983. Combined Sr-O isotope relationships and petrogenesis of Andean volcanoes of South America. *Nature* 302, 814–16.

Deruelle B., Medina E. T., Figueroa O. A., Maragano M. C. & Viramonte, J. G. 1995. The recent eruption of Lascar volcano (Atacama-Chile, April 1993): petrological and volcanological relationships. *Comptes Rendus de l'Academie des Sciences, Serie II* 321 (5), 377–84.

de Silva, S. L. 1989. Geochronology and stratigraphy of the ignimbrites from the 21.30S to 23.30S portion of the Central Andes of Northern Chile. *Journal of Volcanology and Geothermal Research* 37, 93–131.

de Silva, S. L., Self, S., Francis, P. W., Drake, R. E. & Ramirez R., C. 1994. Effusive silicic volcanism in the Central Andes: The Chao dacite and other young lavas of the Altiplano–Puna Volcanic Complex. *Journal of Geophysical Research B* 99 (9), 17805–25.

de Silva, S. L. & Francis, P. W. 1991. *Volcanoes of the Central Andes.* New York: Springer-Verlag.

de Silva, S. L. & Gosnold, W. D. 2007. Episodic construction of batholiths: Insights from the spatio-temporal development of an ignimbrite flare-up. *Journal of Volcanology and Geothermal Research* 167 (3), 320–35.

Ducea, M. 2001. The California Arc: thick granitic batholiths, eclogite residues, lithospheric-scale thrusting, and magmatic flare-ups. *GSA Today* 11, 4–10.

Dilles, J. H. & Wright, J. E. 1988. The chronology of early Mesozoic arc magmatism in the Yerington district of western Nevada and its regional implications. *Geological Society of America Bulletin* 100, 644–52.

Duncan, R. A. & Hogan, L .G. 1994. Radiometric dating of young MORB using ^{40}Ar-^{39}Ar incremental heating method. *Geophysical Research Letters* 21 (18), 1927–30.

Evernden, J. F. & Kistler, R. W. 1970. Chronology of emplacement of Mesozoic batholithic complexes in California and western Nevada. *United States Geological Survey Professional Paper* 623.

Feeley, T. C., Davidson, J. P. & Armendia, A. 1993. The volcanic and magmatic evolution of Zone. *Journal of Volcanology and Geothermal Research* 54, 221–45.

Feeley, T. C. & Davidson, J. P. 1994. Petrology of calc-alkaline lavas at Volcán Ollagüe and the origin of compositional diversity at Central Andean Stratovolcanoes. *Journal of Petrology* 35 (5), 1295–340.

Francis, P. W. & Hawksworth, C. J. 1994. Late Cenozoic rates of magmatic activity in the Central Andes and their relationships to continental crust formation and thickening. *Journal of the Geological Society, London* 151, 845–54.

Galli-Oliver, C. 1967. Pediplain in northern Chile and the Andean uplift. *Science* 158, 653–5.

Gans, P. B., Mahood, G. A. & Schermer, E. 1989. Synextensional magmatism in the Basin and Range Province: a case study from the eastern Great Basin. *Geological Society of America Special Paper* 233.

Gardner, J. N., Goff, F., Garcia, S. & Hagan, R. C. 1986. Stratigraphic relations and lithologic variations in the Jemez volcanic field, New Mexico. *Journal of Geophysical Research B* 91 (2), 1763–78.

Giese, P. 1994. Geothermal structure of the Central Andean crust: implications for heat transport and rheology. *In* Ruetter, K. J., Scheuber, E. & Wigger, P. J. (eds) *Tectonics of the southern Central Andes; structure and evolution of an active continental margin*, 69–76. Berlin, Germany: Springer-Verlag.

Glazner, A. F., Bartley, J. M., Coleman, D. S., Gray, W. & Taylor, R. Z. 2004. Are plutons assembled over millions of years by amalgamation from small magma chambers? *GSA Today* 14 (4/5), 4–11.

Graeber, F. M. & Asch, G. 1999. Three-dimensional models of P waves velocity and P-to-S velocity ratio in the southern central Andes by simultaneous inversion of local earthquake data. *Journal of Geophysical Research B* 104 (9), 20237–56.

Gregory-Wodzicki, K. M. 2000. Uplift history of the Central and Northern Andes: A review. *Geological Society of America Bulletin* 112 (7), 1091–105.

Grunder, A. L. 1995. Material and thermal roles of basalt in crustal magmatism: Case study from eastern Nevada. *Geology* 23(10), 952–6.

Grunder, A. L. 1997. Report on the Miocene to Recent volcanic rocks from the eastern margin of the project area. *In* Tomlinson, A. et al. (eds) *Proyecto de Estudio Geológico de la Franja Longitudinal entre Quebrada Blanca y Chuquicamata, Fase I.* SERNAGEOMIN de Chile report to Coldelco.

Gustafson, L. B., Orquera, W., McWilliams, M., Castro, M., Olivares, O., Rojas, G., Maluenda, J. & Mendez, M. 2001. Multiple centers of mineralization in the Indio Muerto District, El Salvador, Chile. *Economic Geology* 96 (2), 325–50.

Haberland, C. & Rietbrock, A. 2001. Attenuation tomography in the western Central Andes; a detailed insights into the structure of a magmatic arc. *Journal of Geophysical Research B* 106(6), 11,151–67.

Harmon, R. S., Barreiro, B. A., Moorbath, S., Hoefs, J. & Francis P. W. 1984. Regional O, Sr- and Pb-isotopic relationships in late-Cenozoic calcalkaline lavas of the Andean Cordillera. *Journal of the Geological Society, London* 141, 803–22.

Hildreth, W. & Moorbath, S. 1988. Crustal contributions to arc magmatism in the Andes of Central Chile. *Contributions to Mineralogy and Petrology* 98, 455–89.

Hildreth, W. & Lanphere, M. A. 1994. Potassium-argon geochronology of a basalt-andesite-dacite arc system: The Mt. Adams volcanic field, Cascade Range of southern Washington. *Geological Society of America Bulletin* 106, 1413–29.

Hildreth, W., Fierstein, J. & Lanphere, M. A. 2003. Eruptive history and geochronology of the Mount Baker volcanic field, Washington. *Geological Society of America Bulletin* 115 (6), 729–64.

James, D. E. 1981. Role of subducted continental material in the genesis of calc-alkaline volcanics of the Central Andes. *Geological Society of America Memoir* **154**, 769–90.

Johnson, D. M., Hooper, P. R. & Conrey, R. M. 1999. XRF analysis of rocks and minerals for major and trace elements on a single low dilution Li-tetraborate fused bead. *Advances in X-ray Analysis* **41**, 843–67.

Kistler, R. W. & Fleck, R. J. 1994, Field guide for a transect of the central Sierra Nevada, California: Geochronology and isotope geology. *US Geological Survey Open File Report* **94–267**.

Kistler, R. W., Chappell, B. W., Peck, D. L. & Bateman, P. C. 1986. Isotopic variation in the Tuolumne Intrusive Suite, central Sierra Nevada, California. *Contributions to Mineralogy and Petrology* **94**, 205–20.

Klemetti, E. K. 2005. *Constraining the magmatic evolution of the Andean arc at 21° S using the volcanic and petrologic history of Volcán Aucanquilcha, Central volcanic zone, northern Chile.* Ph.D. Dissertation, Oregon State University, USA.

Klemetti, E. K. & Grunder, A. L. 2008. Volcanic evolution of Volcán Aucanquilcha, a long-lived, dacite volcano in the Central Andes of Northern Chile. *Bulletin of Volcanology* **70**(5), 633–50.

Koppers, A. 2002. ArArCALC; software for $^{40}Ar/^{39}Ar$ age calculations. *Computers and Geosciences* **28** (5), 605–19.

Laul, J. C. 1979. Neutron activation analysis of geological materials. *Atomic Energy Review* **17** (3), 603–95.

Le Bas, M. J., Le Maitre, R. W., Streckeisen, A. & Zanettin, B. A. 1986. Chemical classification of volcanic rocks based on the total alkali-silica diagram. *Journal of Petrology* **27** (3), 745–50.

Lipman, P. W. 1984. The roots of ash-flow calderas in western North America: Windows into the tops of granitic batholiths. *Journal of Geophysical Research* **89**, 8801–41.

Lipman, P. W. 2000. Central San Juan caldera cluster: regional volcanic framework. *In* Bethke, P. M. & Hay, R. L. (eds) *Ancient Lake Creede: Its Volcano-Tectonic Setting, History of Sedimentation, and Relation to Mineralization in the Creede Mining District. Geological Society of America Special Paper* **346**, 9–70.

Lipman, P. W. 2007. Incremental assembly and prolonged consolidation of Cordilleran magma chambers: Evidence from the southern Rocky Mountain volcanic field. *Geosphere* **3**, 42–70.

Longo, A. A. 2005. *Evolution and volcanism and hydrothermal activity in the Yanacocha Mining District, northern Perú.* Ph.D. Dissertation, Oregon State University, USA.

Lowenstern, J. B., Persing, H. M., Wooden, J. L., Lanphere, M. A., Donnelly Nolan, J. M. & Grove, T. L. 2000. U-Th dating of single zircons from young granitoid xenoliths: new tools for understanding volcanic processes. *Earth and Planetary Science Letters* **183**, 291–302.

McDonough, W. F. & Sun, S. S. 1995. The composition of the Earth. *Chemical Geology* **120** (3–4), 223–53.

McKee, C. M. 2001, *Volcanology and petrology of Volcán Miño, Andean central volcanic zone'.* Master's Thesis, Oregon State University, USA.

McNulty, B. A., Tong, W. & Tobisch, O. T. 1996. Assembly of a dike-fed magma chamber: The Jackass Lakes pluton, central Sierra Nevada, California. *Geological Society of America Bulletin* **108** (8), 926–40.

Marsh, T. M., Einaudi, M. T. & McWilliams, M. 1997. $^{40}Ar/^{39}Ar$ geochronology of Cu-Au and Au-Ag mineralization in the Potrerillos District, Chile. *Economic Geology* **92** (7/8), 784–806.

Mathieu, L., van Wyk de Vries, B., Holohan, E. P. & Troll, V. R. 2008. Dykes, cups, saucers and sills: analogue experiments on magma intrusion into brittle rocks. *Earth Planetary Science Letters.* doi:10.1016/jepsl2008.02.020

Mattinson, J. M. 1977. Emplacement history of the Tatoosh volcanic-plutonic complex, Washington: Age of zircons. *Geological Society of America Bulletin* **88**, 1509–14.

Miller, J. S., Matzel, J. E. P., Miller, C. F., Burgess, S. D. & Miller, R. B. 2007. Zircon growth and recycling during assembly of large, composite arc plutons. *Journal of Volcanology and Geothermal Research* **167**, 282–99.

Pitcher, W. S. 1978. The anatomy of a batholith. *Journal of the Geological Society, London* **135**, 157–82.

Ramirez, C. F. & Huete, C. 1981. Hoja Ollagüe, region de Antofagasta: SERNAGEOMIN, Carta Geol. de Chile 40, scale 1:250,000, 47 p.

Reid, M. R., Coath, C. D., Harrison, T. M. & McKeegan, K. D. 1997. Prolonged residence times for the youngest rhyolites associated with Long Valley Caldera: 230Th-238U ion microprobe dating of young zircons. *Earth and Planetary Science Letters* **150**, 27–39.

Richards, J. P., Boyce, A. J. & Pringle, M. S. 2001. Geologic evolution of the Escondida Area, Northern Chile: A model for spatial and temporal localization of porphyry Cu mineralization. *Economic Geology* **96** (2), 271–306.

Richards, J. P. & Villeneuve, M. 2001. The Llullaillaco volcano, northwest Argentina: construction by Pleistocene volcanism and destruction by sector collapse. *Journal of Volcanology and Geothermal Research* **105**, 77–105.

Rogers, G. & Hawkesworth, C. J. 1989. A geochemical traverse across the North Chilean Andes: evidence for crust generation from the mantle wedge. *Earth and Planetary Science Letters* **91**, 271–85.

Sawyer, D. A., Fleck, R. J., Lanphere, M. A., Warren, R. G., Broxton, D. E. & Hudson, M. R. 1994. Episodic caldera volcanism in the Miocene southwestern Nevada volcanic field: Revised stratigraphic framework, 40Ar/39Ar geochronology, and implications for magmatism and extension. *Geological Society of America Bulletin* **106**, 1304–18.

Schilling, F., Partzsch, G. M., Brasse, H. & Schwarz, G. 1997. Partial melting below the magmatic arc in the Central Andes deduced from geoelectromagnetic field experiments and laboratory data. *Physics of the Earth and Planetary Interiors* **103** (1–2), 17–31.

Schmitz, M., Heinsohn, W.-D. & Schilling, F. R. 1997. Seismic, gravity and petrological evidence for partial melt beneath the thickened Central Andean crust (21–23S). *Tectonophysics* **270**, 313–26.

Schwarz, G. & Krueger, D. 1997. Resistivity cross section through the southern Central Andes as inferred from magnetotelluric and geomagnetic deep soundings. *Journal of Geophysical Research B* **102** (6), 11957–78.

Trumbull, R. B., Wittenbrink, R., Hahne, K., Emmermann, R., Busch, W., Gerstenberger, H. & Siebel, W. 1999. Evidence for Late Miocene to Recent contamination of arc andesites by crustal melts in the Chilean Andes (25–26S) and its geodynamic implications. *Journal of South American Earth Sciences* **12**, 135–55.

Vergara, H. 1978. Cuadrangulo Quehita y sector occidental del cuadragulo volcán Miño, Región de Tarapacá. Santiago Instituto de Investigaciones Geológicas, Carta Geológica de Chile (1:50,000) **31**, pp. 1–44.

Wenner, J. M., & Coleman, D. S. 2004. Magma mixing and Cretaceous crustal growth: Geology and geochemistry of grantites in the central Sierra Nevada Batholith, California. *International Geology Review* **46**, 880–903.

White, S. M., Crisp, J. A. & Spera, F. J. 2006. Long-term volumetric eruption rates and magma budgets. *Geochemistry, Geophysics, Geosystems* **7** (3) doi:10.1029/2005GC001002.

Wiebe, R. A. 1996. Mafic-silicic layered intrusions: The role of basaltic injections on magmatic processes and the evolution of silicic magma chambers. *Transactions of the Royal Society of Edinburgh: Earth Sciences* **87**, 233–42.

Wigger, P. J., Schmitz, M., Araneda, M., Asch, G., Baldzuhn, S., Giese, P., Heinsohn, W.-D., Martinez, E., Ricaldi, E., Rower, P. & Viramonte, J. 1994. Variation in the crustal structure of the Southern Central Andes deduced from seismic refraction investigations. *In* Ruetter, K. J., Scheuber, E. & Wigger, P. J. (eds) *Tectonics of the southern Central Andes; structure and evolution of an active continental margin,* 23–48. Berlin, Germany: Springer-Verlag.

Wörner, G., Harmon, R. S., Davidson, J., Moorbath, S., Turner, D. L., McMillan, N., Nye, C., Lopez-Escobar, L. & Moreno, H. 1988. The Nevados de Payachata volcanic region (18S/69W, N. Chile): I. Geological, geochemical, and isotopic observations. *Bulletin of Volcanology* **50**, 287–303.

Wörner, G., Moorbath, S. & Harmon, R. S. 1992. Andean Cenozoic volcanic centers reflect basement isotopic domains. *Geology* **20**, 1103–6.

Wörner, G., Moorbath, S., Horn, S., Entenmann, J., Harmon, R. S., Davidson, J. P. & Lopez-Escobar, L. 1994. Large- and fine-scale geochemical variations along the Andean arc of Northern Chile (17.5–22S). *In* Ruetter, K. J., Scheuber, E. & Wigger, P. J. (eds) *Tectonics of the southern Central Andes; structure and evolution of an active continental margin,* 77–92. Berlin, Germany: Springer-Verlag.

Zandt, G., Velasco, A. A. & Beck, S. L. 1994. Composition and thickness of the southern Altiplano crust, Bolivia. *Geology* **22** (11), 1003–6.

Zellmer, G., Turner, S. P. & Hawkesworth, C. J. 2000. Timescales of destructive plate margin magmatism: new insights from Santorini, Aegean volcanic arc. *Earth and Planetary Science Letters* **174**, 265–81.

ANITA L. GRUNDER, ERIK W. KLEMETTI[1] and CLAIRE M. MCKEE, Department of Geosciences, Oregon State University, Corvallis, OR 97331, USA.
e-mail: grundera@geo.oregonstate.edu
[1]Present address: Department of Geology, 1 Shields Ave, University of California Davis, Davis, CA 95616.
e-mail: klemetti@geology.ucdavis.edu

TODD C. FEELEY, Department of Earth Sciences, Montana State University, Bozeman, MT 59717, USA.